Nano Today 50 (2023) 101837

Contents lists available at ScienceDirect

Nano Today

journal homepage: www.elsevier.com/locate/nanotoday

Carbon dots as oxidant-antioxidant nanomaterials, understanding the structure-properties relationship. A critical review

Plinio Innocenzi [a,b,*], Luigi Stagi [a]

[a] Laboratory of Materials Science and Nanotechnology (LMNT), Department of Biomedical Sciences, CR-INSTM, University of Sassari, Viale San Pietro 43B, 07100 Sassari, Italy
[b] College of Science, Department of Chemistry. United Arab Emirates University, Al Ain, United Arab Emirates

ARTICLE INFO

Article history:
Received 7 December 2022
Received in revised form 8 February 2023
Accepted 22 March 2023
Available online 30 March 2023

Keywords:
Carbon dots
Graphene quantum dots
Radical scavenging
Reactive oxygen species
Free radicals
Nanoparticles

ABSTRACT

Carbon dots (C-dots) are a large family of nanomaterials characterized by an intense photoluminescence. The origin of the emission is multifaceted and is dependent on a number of factors, including structure, surface, and composition. The term "carbon dots" is quite broad and encompasses a wide range of carbon nanostructures. The multiple properties are a result of this variability, which also makes it difficult to establish a clear structure-property relationship. Photoluminescence is the property of this class of nanomaterials that has garnered the greatest attention due to the possibility of applications in various fields, including biotechnologies, electronics, and energy. Another property of C-dots that has only lately been recognized is their antioxidant activity, i.e., the ability to act as a free radical scavenger. Furthermore, it has been proven that certain types of C-dots function as oxidizing agents when exposed to visible and/or UV radiation. This dual oxidant-antioxidant nature is particularly intriguing and closely related to the C-dot properties. Although many articles have been published on the subject, it still needs to be understood what structure-property relationships regulate the responses to free radicals. This review aims to provide a general overview of the characteristics of C-dots as scavengers or radical emitters by a critical analysis of the relevant studies. Based on their intended application as oxidants or antioxidants, the findings of this review can be used to synthesize C-dots with precisely defined functional properties.

Contents

Introduction . . . 2
The large family of C-dots . . . 2
Graphene quantum dots (GQDs) . . . 2
Carbon quantum dots (CQDs) . . . 3
Carbon nanodots (CNDs) . . . 3
Carbonized polymer dots (CPDs) . . . 3
Reactive oxygen species . . . 3
Understanding the ROS formation in carbon dots . . . 4
The mechanism of ROS generation . . . 5
N-doping effect on ROS generation . . . 6
Doping C-dots with heteroatoms besides N . . . 7
The role of surface functional groups on ROS generation. . . . 7
Ultrasound generation of ROS . . . 9
Design of ROS emitting C-dots. . . . 9
Radical scavenging properties . . . 10
Scavengers of reactive nitrogen species. . . . 10

* Corresponding author at: Laboratory of Materials Science and Nanotechnology (LMNT), Department of Biomedical Sciences, CR-INSTM, University of Sassari, Viale San Pietro 43B, 07100 Sassari, Italy.
E-mail address: plinio@uniss.it (P. Innocenzi).

https://doi.org/10.1016/j.nantod.2023.101837

Nitrogen reactive species scavenging by carbon nanodots (CNDs). . . . 10
Nitrogen reactive species scavenging by graphene quantum dots . . . 11
Scavenging of hydroxyl radicals (·OH) . . . 15
Scavenging of superoxide radical anions ($O_2^{\cdot-}$) . . . 16
Dual oxidant-antioxidant nature of carbon dots . . . 16
Conclusions and future outlooks . . . 17
Funding . . . 18
CRediT authorship contribution statement . . . 18
Data Availability . . . 18
Declaration of Competing Interest . . . 18
References . . . 18

Introduction

Carbon dots (C-dots) are one of the hottest topics of research and object of a growing interest because of their expected applications in photonics [1–5] and biotechnology [6–8]. The potential production low-cost, the lack of toxicity and the low environmental impact have risen the expectations on this class of nanomaterials. In a next future C-dots could replace the semiconductor quantum dots in several cases, taking also the advantage of the high flexibility offered by the synthesis. The C-dots can be finely tuned using organic chemistry that offers many possibilities to control the properties through modification of structure and surface, from the precursor molecule to the nanoparticle [9]. In particular, the surface control is critical for C-dots because most properties are directly affected by any modification in the surface functional groups [10,11]. The C-dots can be considered as dual core-surface structures, where much more than in metallic or semiconductor nanoparticles the surface is critical to control the properties. At the same time, defects are an intrinsic part of the C-dots, and therefore the core-surface-defects combination plays a dramatic role. This is a general description but, however, it should carefully considered that C-dot is a quite broad definition and within this name several types of nanomaterials with so much different properties are included. For instance, some C-dots have a graphitic core structure whose properties are described in terms of quantum mechanics, such as the graphene carbon dots, while many others have just a carbonaceous structure. From this point of view such different nanomaterials could be hardly classified within the same class of materials. One reason they are all regarded as belonging to the C-dot family is that they share the same intrinsic organic nature and, in many cases, show similar properties. This is a critical point that is seldom underlined, but it is likely one of the reasons that has brought to combine materials with so much different structure in the same group. C-dots are characterized by an intense fluorescence, in most of the cases in the blue [12]. This is what has attracted from the very beginning so much attention. This intense fluorescence, however, even if looks similar can have different origins in the various types of carbon dots [13]. The properties of C-dots, as we have just underlined, derive from a complex combination of core structure, defects and surface state that is difficult to generalize. The core structure can be graphitic, or even formed by graphitic carbon nitride g-C_3N_4 [14], amorphous, or a combination of both. At the same time the extension and amount of sp^2 domains play also a very critical role. A combination of fluorescent molecular structures of diverse nature connected to a carbonaceous matrix can form the core structure. The complexity of such structures represents an inherent limitation in the development of C-dot-based applications. Furthermore, there is a strong imbalance between the articles devoted to exploring and develop applications with respect those dedicated to the basic understanding of the properties. Paradoxically, this imbalance is slowing down the very development of applications because without an extremely precise control over the structure and properties, it is difficult to get to their use in areas, such as biotechnologies, where safety standards are very tight. On the other hand, the most attractive properties of C-dots are the intense fluorescence and in some cases phosphorescence [15]. The majority of the research in the field has been dedicated obtaining a high fluorescence quantum yield and shifting the emission in the red region [16,17], which for bio-applications is critical. Recently, however, another characteristic of C-dots has drawn much interest: their capacity to produce radicals and reactive oxygen species. This property can find an immediate application in photodynamic therapy [18]. At the same time, however, it has become clear that beside having oxidant properties under illumination, C-dots can also act as radical scavengers and antioxidants. The possibility of C-dots to act as nanozymes has been, therefore, quickly envisaged [19,20]. The oxidant-antioxidant crossover capability is quite rare [21], and represents another of the big challenges offered by C-dots [22]. Controlling such properties, however, is likely even more difficult than fluorescence, because the structure-properties relationship must be assessed with much detail, a mission that given the intrinsic “chaotic” nature of C-dots appears pretty difficult to accomplish. It should be underlined that most of the work in the field has been concentrated on using graphene quantum dots. A nanosystem with controlled dimension and structure represents an intrinsic advantage with respect to amorphous or polymeric structures, especially when the sp^2 domains are a critical parameter. Even in this case, however, the large variability of the possible nanostructure needs a careful comparative study.

This work is a meta study of the current scientific literature in the field of C-dots that has the purpose to give, through a critical comparison, an overall picture of the structure-properties relationship of the oxidant-antioxidant capability. In the first part will be described for the lectures not familiar with the subject what are carbon dots and what are the reactive oxygen species. The following chapters are instead dedicated to an in-depth analysis of the chemical-physical mechanisms behind the generation of reactive species and the scavenging properties of the dots.

The large family of C-dots

The family of nanomaterials defined as carbon dots consists of a wide variety of carbon-based 0D nanostructures generally characterized by high fluorescence and nanodimensions smaller than 10–20 nm. However, a clear-cut definition is difficult to obtain because of the many structural differences within this group of nanomaterials. The intrinsic “black box” nature of C-dots, whose properties are due to a combination of the core structure and surface composition, can be considered a peculiar characteristic of these nanomaterials. Some classifications of C-dots, mainly based on their core-surface interaction, have been proposed in the scientific literature. On the other hand, the emission can have different origins [23,24], with defects and surface functional groups playing also an important role.

Graphene quantum dots (GQDs)

The graphene quantum dots form an important group of C-dots with a structure of a single or few graphene layers [25,26]. GQSs are

Table 1
Design parameters for graphene quantum dots.

Dimensions	Shape
- Height, less than 10 layers (thickness 1.5 – nm)	- Irregular,
- Lateral size (< 100 nm)	- triangular, hexagonal,
	- circular, polygonal
N-doping	**Heteroatoms doping**
- Pyridinic-N	Mono, double, multiple
- Graphitic-N	(S, Se, F, Cl, P, Na, K, B)
- Pyrrolic-N	
Functional Groups	**Defects**
- Electron donating	- sp^3-like defects
$-NH_2$, -OH, OR', -OCOR'	- Vacancies
- Electron withdrawing	- Disorder of the basal plane
-CHO, =O, -COOR', -COOH, CH, NH_3^+, NO_2	- Free edges

generally synthesised via top-down routes from graphene or other graphitic materials. The photoluminescence originates from a combination of quantum confinement and surface effects due to the functional chemical groups at the edges of the graphene core structure that is mostly formed by sp^2 hybridized carbons.

This group of C-dots has grown in importance as the benefit of having greater control of the properties through precise nanostructure engineering has become more evident. (Table 1). GQDs have a better defined structure than other groups of C-dots whose nature is intrinsically disordered, and can be properly designed as a function of the application. [27]. For this reason, GQDs are favoured over other C-dots, particularly when the nanomaterial response is governed by external stimuli. The GQDs have a characteristic asymmetrical shape, because the number of layers defines the thickness, generally lower than 10, and the later size that does not exceed 100 nm. Besides the dimensions, the properties are also dependent on the shape that within some limits can assume different geometries, such as hexagonal and triangular. The composition is a fundamental parameter as well, and heteroatom (S [28], Se [29], F [30], Cl [31], P [32], B [33], K [34]) and multiple heteroatom [35] doping is a popular strategy to modify the luminescence properties. Doping with N, which in general is a very effective route to increasing or shifting the emission, is another design tool. It introduces different N-sites in the GQDs, pyrrolic-N, pyridinic-N and graphitic-N [36]. Controlling the functional groups is also mandatory, paying attention if they possess electron donating, $-NH_2$, -OH, -OR', -OCOR', or electron drawing nature, -COOH, -CH, NH_3^+, NO_2. Finally, defects, such as sp^3-like defects [37], vacancies [38], free edges [39], which can be easily introduced during top-down syntheses, also affect the properties. The combination of so many parameters make controlling the properties a very challenging task, nevertheless, the design of the application cannot be done without an in-depth comprehension of the basic properties.

The classification becomes more complicated in the case of C-dots that do not have a full graphenic structure. Two different nanostructures can be observed, C-dots with a completely amorphous core and those with a partially graphitic structure. The origin of the fluorescence in these cases is different, and for this reason, it is better to divide this type of dots, characterized by a structure that is not purely graphenic such as GQDs, into two groups: the carbon quantum dots (CQDs) [40] and the carbon nanodots (CNDs). This classification can cause some confusion because not all the researchers in the field always follow this way of referring to C-dots by their structure. The definition leaves, in fact, some room for ambiguities when the generic term carbon dots is used.

Carbon quantum dots (CQDs)

The CQDs are characterized by a graphitic crystalline core structure, mainly composed of sp^2 hybridized atoms, and a carbonaceous sp^3 surface containing oxygen and nitrogen-based functional groups [41]. The quantum confinement within the graphitic core controls the luminescence that can be tuned by modulating the size and surface functionalization. The quasi-spherical shape of CQDs also marks one of the differences with respect to GQDs that, instead, have one dimension, the height that is controlled by the number of graphene fragment layers and therefore smaller than the lateral size. Aside from being graphitic, the crystalline core structure can also be formed in some cases by carbon nitride, g-C_3N_4 [42].

Carbon nanodots (CNDs)

The C-dots that have an amorphous carbonized core form another sub-group of this family of nanomaterials. In the case CNDs, carbon is most in the sp^3 state, even if sp^2 domains can form in the nanodots. The photoluminescence is not controlled by quantum confinement effects, while residual molecular fluorophores that form during the synthesis are at the main origin of the fluorescence [43–45]. Fluorescent molecules can readily form as a by-product of the synthesis and can be present at a different extent in CQDs, mainly around the graphitic core, while in the CNDs they are evenly distributed within the particle. The distinction between CQDs and CNDs is quite tricky because, in many cases, tiny graphitic clusters can be present in the particles, and an in-between situation can easily occur. In CNDs, the molecular fluorophores that form as by product of the pyrolysis are at the origin of the emission, in particular in the blue range.

Carbonized polymer dots (CPDs)

Carbonized polymer dots are another type of C-dot that form when amorphous carbon and polymers cross-link to form a hybrid structure. (CPDs) [46]. Surface states, molecular fluorophores, and crosslink enhanced emission [47] are all factors that contribute to the emission.

To complicate any attempt at rational classification, it should be noted that organic polymers can also form fluorescent nanoparticles known as polymer dots (PDs). They do not contain any crystalline or carbonaceous amorphous structure and can be considered for this reason as a distinct family.

The C-dot structure's high degree of diversity thus reveals how challenging it is to define a generic structure-properties relationship (Fig. 1). When looking at emission sources, we should consider not only the structure, dimension, composition, and surface, but also, as we have seen, the presence and extension of defects. To summarize, the main mechanisms at the root of the photoluminescence are:

1. Quantum confinement effects correlated to the presence of π-conjugated domains in the core.
2. Emission from molecular fluorophores.
3. Photoluminescence induced by defects, surface states, and doping.
4. Emissions involving triplet states that can produce thermally delayed fluorescence or phosphorescence.

These mechanisms can also work in synergy, and a clear correlation with specific structural properties of the C-dots is, in any case, quite difficult.

Reactive oxygen species

The generation of radicals and, more generally, reactive oxygen species (ROS) is a natural event that underlies several biological processes [48]. An excess of such species generates, however, oxidative stresses responsible of several serious diseases because an unbalanced production of ROS can result in a severe damage of the

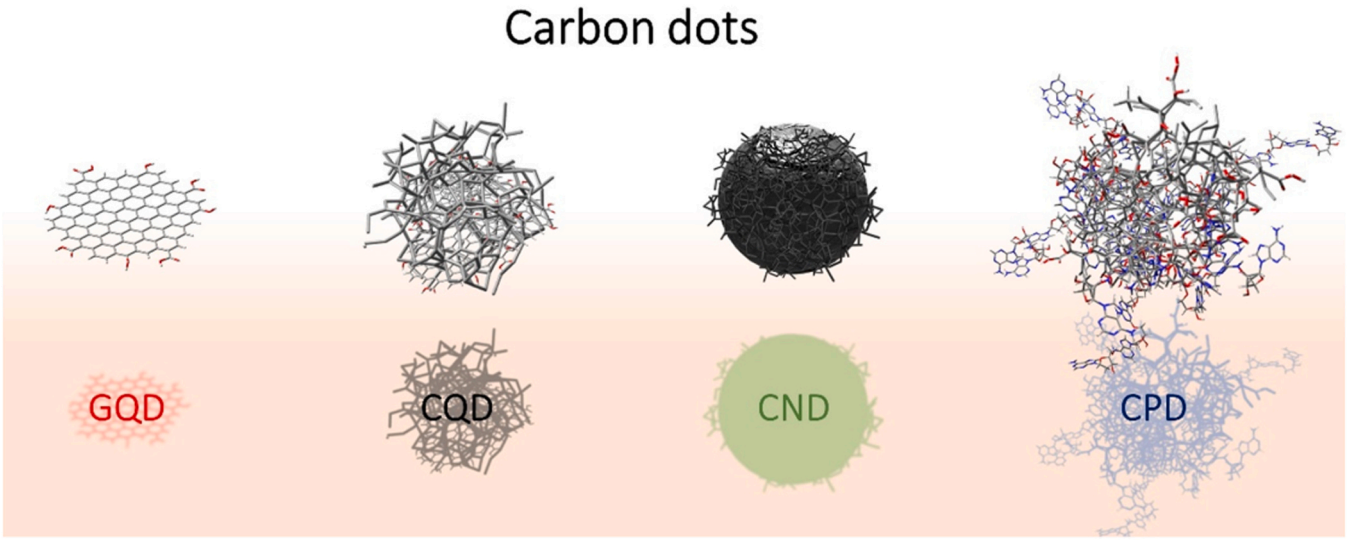

Fig. 1. Schematic drawing of the different structures of carbon dots: Graphene quantum dots (GQD), Carbon quantum dots (CQD), Carbon nanodots (CND) and Carbon polymer dots (CPD).

cells [49]. High amounts of ROS or oxidants create a disequilibrium in the cell capability of producing an effective antioxidant response, a situation that defines the oxidative stress.

Even if ROS can have toxic effects on cells, the controlled formation of reactive species can be used as an active tool for antibacterial and antiviral applications or in photodynamic therapy. Some carbon nanomaterials present an interesting dual response to reactive species, they can act as scavengers, so reducing the number of free radicals and ROS, or can generate under irradiation reactive species by themselves. This dual nature is not observed in single molecule antioxidants, such as ascorbic acid, and is instead a distinctive and intriguing property of several carbon nanomaterials. C-dots, in particular, can exhibit both antioxidant and oxidant responses. The arise of these properties is, however, correlated with the synthesis and processing pathway and cannot be considered a general property of carbon dots by themself.

Because oxygen has a couple of unpaired electrons in the outer valence shell is highly susceptible to form reactive species. The ROS can be both free radical oxygen intermediates such as hydroxyl radicals $^{\bullet}OH$, superoxide anions $^{\bullet}O_2^-$, or non-free radicals as hydrogen peroxide H_2O_2 and singlet oxygen $^1O_2$ [50].

The reduction of molecular oxygen gives the superoxide anions, $O_2^{\bullet-}$, one of the most reactive species through:

$$O_2 + e^- \rightarrow O_2^{\bullet-} \quad (1)$$

On turn, the dismutation of the superoxide anion forms hydrogen peroxide and molecular oxygen:

$$2\,O_2^{\bullet-} + 2\,H^+ \rightarrow H_2O_2 + O_2 \quad (2)$$

while the partial reduction of hydrogen peroxide gives hydroxide ions and hydroxyl radicals ($^{\bullet}OH$), or water after its full reduction: (3).

$$H_2O_2 + e^- \rightarrow HO^- + {}^{\bullet}OH$$

$$2\,H^+ + 2\,e^- + H_2O_2 \rightarrow 2\,H_2O \quad (3)$$

Another ROS that is a strong oxidant is singlet oxygen, $^1O_2$, which is not a radical but an excited state of molecular oxygen O_2 that in the ground state is characterized by two single-occupied antibonding orbitals, π_x^* and π_y^*, with electrons having parallel spins [51]. The energetically near electronic states, the excited $^{1\Sigma+}_{g}$ and $^1\Delta_g$ singlet states as well as the $^{3\Sigma-}_{g}$ triplet ground state are, therefore, the result of this peculiar molecular arrangement. The metastable singlet oxygen, the $^1O_2(^1\Delta_g)$ state, has both the electrons coupled in a single orbital and has a lower energy but significantly longer lifetime than the $^{1\Sigma+}_{g}$ excited state (Fig. 2).

In the singlet excited state the spin is still unpaired as in the ground state but the two electrons occupy distinct antibonding orbitals. In the triplet excited state, the energy level is higher than the excited singlet state and the electrons still occupy two distinct antibonding orbitals but this time the spin is paired.

The formation of $^1O_2$ is generally observed through energy transfer to molecular oxygen in its triplet ground state, $^3O_2$. This process can be mediated by photosensitisers that absorb light at a specific wavelength and transfer the energy from their excited state to $^3O_2$, activating the formation of $^1O_2$. Compared to other free radicals, the lifetime of singlet oxygen in the air is longer and has been measured to reach 2.80 s at 23 °C under 1 atm [52]. In this span of time $^1O_2$ diffuses in the air about 0.992 cm while in water the diffusion length is reduced to 200 nm [53].

The photosensitization of $^3O_2$ via energy transfer is a process that is relatively easy to occur. In fact, if we compare the energy required to excite $^3O_2$ to the $^{1\Sigma+}_{g}$ and $^1\Delta_g$ states, 156.9 and 94.14 kJ mol^{-1}, respectively, this is lower than most of the energies of the excited triplet states of many organic molecules that can act as photosensitizers absorbing light. Longer is the average lifetime in the excited state and higher is the possibility of intermolecular interaction and energy transfer to $^3O_2$. On the other hand, molecules whose excited states are lower than $^{1\Sigma+}_{g}$ and $^1\Delta_g$ in molecular oxygen, are able to quench these states via electronic energy transfer. This process, on turn, reflects in the formation of an excited state of the quencher.

Regarding the photosensitized reactions that involve oxygen they have been divided into *Type I* and *Type* oxidation [54]. The reaction pathway depends on the properties of the sensitizer, *Type I* undergoes photoinduced electron transfer with formation of $O_2^{\bullet-}$ and $HO^{\bullet}$. The *Type II* photoprocess involves, instead, the energy transfer from the sensitizer to oxygen in the ground triplet state, $^3O_2$ (Fig. 3).

Understanding the ROS formation in carbon dots

Understanding the chemical and physical mechanisms underlying ROS generation in C-dots is certainly necessary to accurately design the functional properties. One of the major difficulties is related to the exact knowledge of the structure, which is formed by the core and functional groups. majority of the studies have focused on

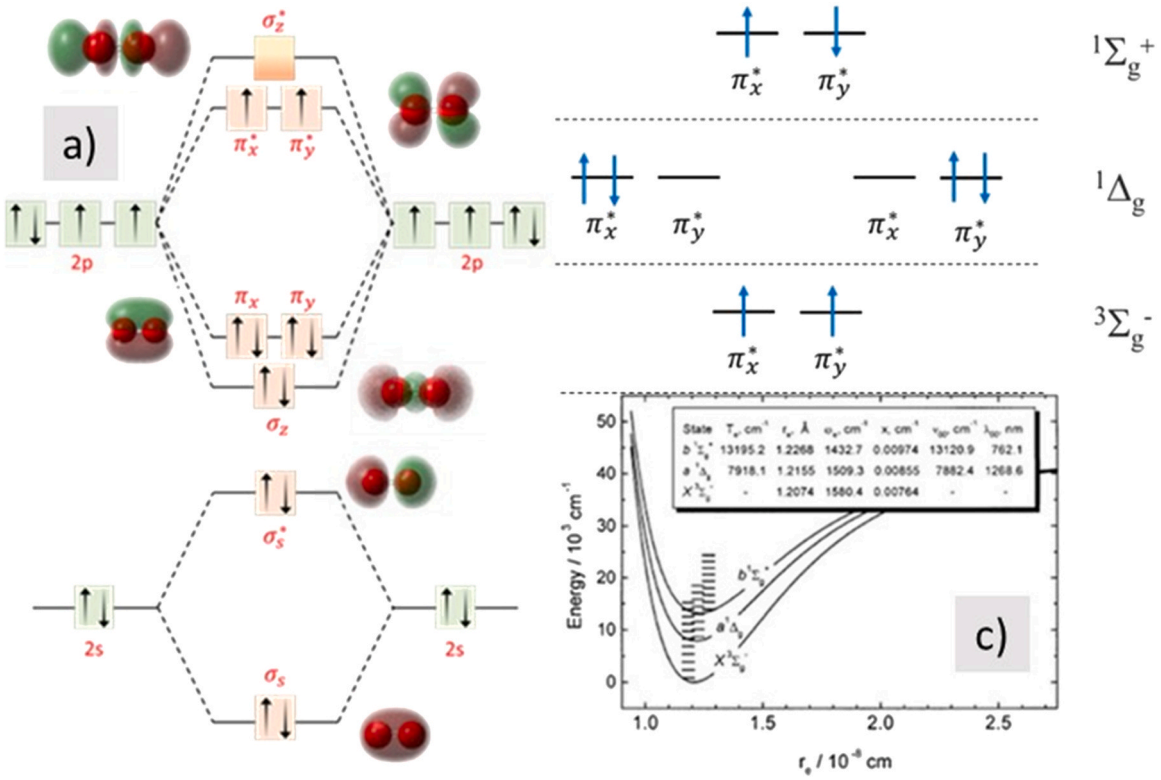

Fig. 2. a) The molecular oxygen electronic configuration. b) The electronic configuration of the antibonding orbitals excited states in molecular oxygen. c) Potential energy curves of the three lowest electronic states of O_2.
Reproduced with permission from ref. [51]

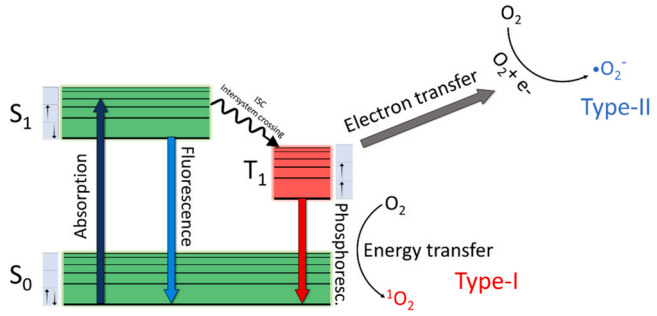

Fig. 3. Schematic of the photophysical processes indicated as *Type I* (energy transfer to oxygen in the ground state) and *Type II* (electron transfer to oxygen in the ground state).

the most common ROS, namely singlet oxygen, hydroxyl radicals, and the superanion radicals. The comparative analysis of the results published so far, although it does not allow reconstructing a general picture, nevertheless shows some salient features. One of these is that the generation of radicals by C-dots is highly structure-dependent and very specific. Therefore, only in limited cases a particular C-dot generates all the different types of ROS. The mechanisms of radical generation are, in fact, different, and this requires designing and synthesizing the C-dot on purpose. Another point to note is that most of the published work focuses on GQDs. This type of particle has the advantage of having a structure that is easier to characterize and model.

The mechanism of ROS generation

The photostimulated generation [51] of $^1O_2$ in carbon based nanomaterials is well documented for different nanostructures, in particular fullerenes [55,56], graphene [57–59] and carbon nanotubes [60]. The carbon nanomaterials work as sensitizers for the production of singlet oxygen that finds applications in nanomedicine, in particular photodynamic therapy [61].

Some C-dots, may act as photosensitizers by promoting ground state electrons into an excited singlet state. that undergoes intersystem crossing (ISC) to a more stable excited triplet state via an energy transfer process to oxygen molecules. The whole process, indeed, results in the formation of excited oxygen in singlet state $^1O_2$ that, as we have seen, is extremely reactive due to the spin pairing of the two electrons in the π^* antibonding orbitals (Fig. 2). Fig. 4.

GQDs produced with polythiophene as a precursor, however, have been linked to a distinct multistate photosensitization mechanism [62]. In conventional sensitizers for photodynamic therapy, such as porphyrines [63] and phtalocyanines [64], $^1O_2$ is generated by energy transfer from the excited triplet state of the sensitiser (T_1) to $^3O_2$. In these systems the singlet oxygen quantum yield (QY), defined as the number of $^1O_2$ generated per single photon, is generally lower than ~1. In the GQDs prepared from polythiophene via hydrothermal synthesis, the QY shows a value beyond 1 up to ~1.3 that can be explained only if a new excitation mechanism is occurring. Because the calculated energy gaps, ground state (S_0) - excited singlet state (S_1), and ground state (S_0) - excited triplet state (T_1), in CQDs are both larger than the energy of formation of $^1O_2$, a multistep mechanism has been used to explain the high quantum yield (Fig. 5).

The energy transfer to $^3O_2$ to give $^1O_2$ can happen through two different decay pathways. The first “conventional” one, via energy transfer from the excited triplet state, T_1, to the ground state S_0 (Eq. 1). In this stage, the energy transfer to $^3O_2$ is allowed even if the transition from the excited singlet state, S_1, to T_1, is in general a non-radiative process and the energy transfer should not occur.

$$T_1 + O_2\ (^3\Sigma_g^-) \rightarrow S_0 + O_2\ (^1\Delta_g) \quad (4)$$

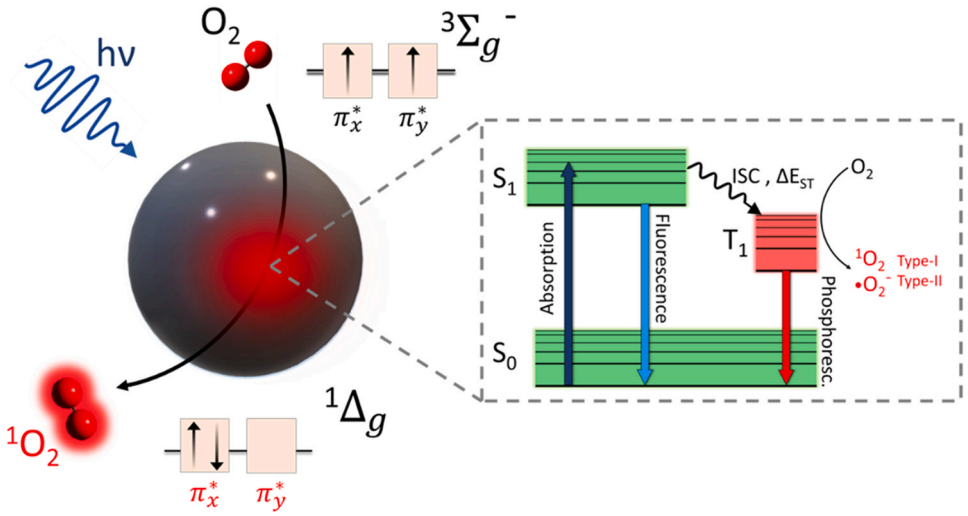

Fig. 4. Generation of singlet oxygen through a photosensitizer.

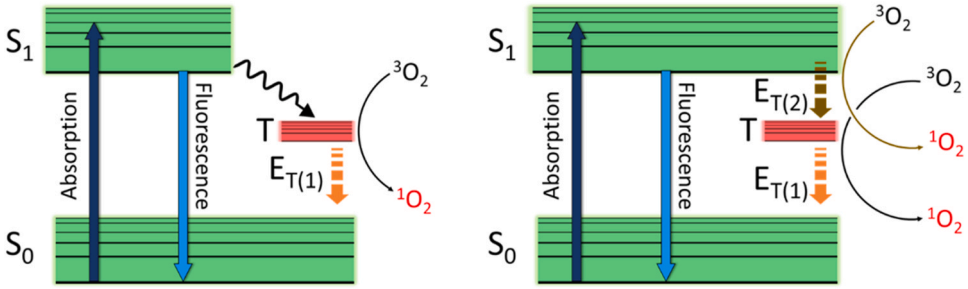

Fig. 5. Schematic illustration of the $^1O_2$ generation mechanisms by conventional photodynamic therapy agents (left) and GQDs (right). Redrawn from ref. 62.

In the second one the energy is transferred, instead, from the excited singlet state, S_1, to triplet excited state, T_1:

$$S_1 + O_2 (^{3\Sigma}_{g}) \rightarrow T_1 + O_2 (^1\Delta_g) \quad (5)$$

Both the energy gaps, $\Delta E_{T1\text{-}S0}$ and $\Delta E_{S1\text{-}T1}$ are large enough, suggest the authors, to allow the excitation of $^3O_2$. In this way the energy transfer to $^3O_2$ can happen during the decay from the excited singlet state to the triplet excited state and during the decay to the ground state, increasing the QY of $^1O_2$ and explaining the $^1O_2$ larger than one.

The GQDs derived from phthalocyanines do not emit any ROS species in the dark, while when excited with visible light (568 nm) generates $^1O_2$. The GQDs are able to absorb visible light in the 400–700 nm range and exhibit an emission peaking at 680 nm in the deep red.

C-dots prepared via solvothermal reaction of citric acid and 1,5-diaminenaphtalene generate $^1O_2$ upon activation by visible light[65]. The absorption of a $^1O_2$ quencher, 1,3-diphenylisobenzofuran, is reduced when the solution containing the C-dots is irradiated by a laser light at 532 nm. The data show a 32% reduction of the 1,3-diphenylisobenzofuran absorbance at 410 nm after 22 min, which suggests a moderate formation of singlet oxygen. This property has been exploited for in vitro antibacterial photodynamic inactivation. The generation of ROS upon irradiation by visible light in this type of C-dots is limited to $^1O_2$ while $O_2^{\bullet-}$ or $^{\bullet}OH$ do not form.

The two previous examples show that the capability of C-dots to generate ROS depends on the different photoreaction pathways. The dots that exhibit an efficient energy transfer to $^3O_2$ not necessarily have at the same time the capability of transferring electrons. The two phenomena are well distinct and depend on the C-dots structure and composition. In some cases, multiple formation of different ROS is, however, also observed. At the same time, as a function of the excitation energy levels, different mechanisms of energy transfer are also possible. They will be briefly analyzed and discussed in the next paragraphs.

Doping with nitrogen is one of the most widely used methods to modify the properties of C-dots and has also been applied to increase the $^1O_2$ generating capability.

N-doping effect on ROS generation

One of the most common methods for modulating the properties of C-dots is nitrogen doping, which has also been used to boost the ability to generate $^1O_2$ [66–69]. Several precursors containing nitrogen, such as ethylenediamine [70,71], urea or 1,5-diaminenaphthalene, have been employed in the synthesis of C-dots to incorporate nitrogen atoms. Furthermore, the presence of N is often accompanied with the formation of oxygen functional groups that also modify the material properties.

N-doping creates different types of chemical bonding within the graphene layers in GQDs: *graphitic-N* located at the core or edge sites (N is interconnected with three C atoms at the core or two carbon atoms at edge sites of graphene-like structures); *pyridinic-N* (N interconnected with two C atoms at the edge); *pyrrolic-N* (N interconnected with two p electrons and conjugated to a π bonding system); *edge* and *surface amines* (Fig. 6).

Because different N-sites would develop to various degrees, it is challenging to control. In general, higher N contents shift to red both the absorption and emission, while also the electronic properties change with respect to the undoped carbon dots. Computational modelling has demonstrated that graphitic-N sites cause red-shift

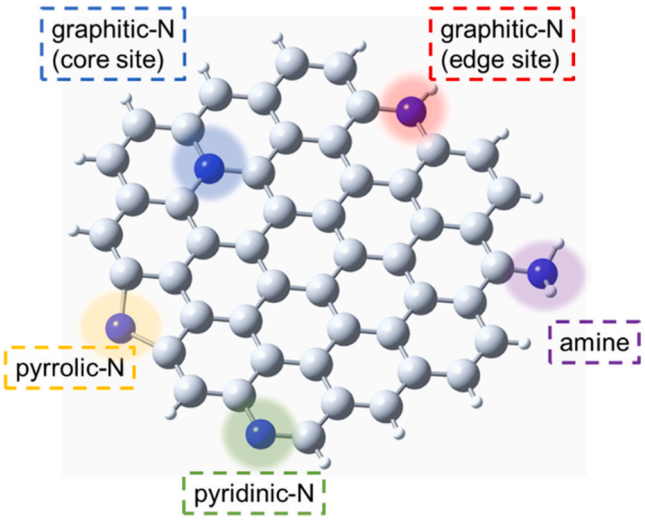

Fig. 6. Common types of N-doping/functionalization in N-doped C-dots.

because they narrow the HOMO-LUMO energy gap by filling the unoccupied π^* orbitals of a conjugated system with the excess electrons [72]. On the other hand, pyrrolic and pyridinic-N sites vice versa cause a blue shift; the opposite response of the different N-sites indicates that the position of the nitrogen atoms within the graphenic structure is a key parameter to take into account.

A systematic investigation on the effect of the different N-sites in GQDs to generate ROS has been done by Wu et al. [73]. A first finding is that the generation of ROS from GQDs prepared by citric acid and ethylenediamine using a hydrothermal route depends on the amount on N sites and it has a peculiar trend. Samples prepared with increasing amounts of ethylenediamine, the source of nitrogen, exhibit a higher fluorescence quantum yield and a larger decay time that increase in accordance with the N content (Table 1).

The photosensitization effect, however, is not linear and shows a maximum at a specific composition (Fig. 7) (citric acid: ethylenediamine = 1: 1, in molar ratio). The N-pyridinic species increases when ethylenediamine concentration rises, whereas the N-pyrrolic and N-graphitic species decrease. The maximum production of ROS, therefore, corresponds to the highest content in pyrrolic-N and graphitic-N sites and a minimum in pyridinic-N sites. The variations in N-sites accurately represent the GQDs' capacity to produce ROS, particularly $^1O_2$ and $O_2^{\cdot-}$, without actually producing any $^{\cdot}OH$. The authors have performed some theoretical calculations, using simplified models of N-CDs based on coronene and pyrene-like structures.

The computations have demonstrated that the graphitic-N sites in both coronene and pyrene-like N-doped structures exhibit the lowest energy difference between the excited singlet state and the excited triplet (ΔE_{ST}) state (Table 2). The decrease in ΔE_{ST}, and HOMO-LUMO band gap causes an optical red shift that results in a higher photosensitization because a smaller band gap favours the ISC and the activation of the triplet state. The data of the ΔE_{ST} simulation show, however, that while graphitic-N sites reduce the gap, pyrrolic-N produces the opposite effect.

The experimental photosensitization efficiency of the N-doped C-dots is correlated also with the pyrrolic-N sites. The singlet oxygen generation depends not only by the energy transfer from its triplet excited state to O_2 but also on the interaction between the photosensitizer and the molecular oxygen. The same authors have used again the coronene-pyrene N-site model to obtain theoretical values of oxygen adsorption on the different structures (Table 2). A thermal treatment of the CDs changes the relative content of N-sites, with a decrease of pyridine-N and a rise of graphitic and pyrrolic-N (Table 2). The oxygen sensitization capability increases in accordance and samples with the highest content of graphitic and pyrrolic N-sites have also the highest efficiency. The adsorption energy of oxygen on different nitrogen doping structures follows the order: *pyrrolic N > pyridinic N > graphitic N*.

Another experimental observation is that the pyrrolic and graphitic N-sites act as electron donating groups and favour the electron transfer to the adsorbed $^3O_2$ to form $O_2^{\cdot-}$. The citric acid – ethylenediamine dots, therefore, generate not only singlet oxygen but also superoxide anions (Fig. 7). As we have seen, the formation of singlet oxygen is a process involving an energy transfer, while $O_2^{\cdot-}$ should form via electron transfer.

$^3O_2 + (h\nu + CQD^*)$ (energy transfer) $\rightarrow$ $^1O_2$ (singlet oxygen)

$^3O_2 + (h\nu + CQD^*)$ (electronic transfer) $\rightarrow$ $O_2^{\cdot-}$ (superoxide anions)

This suggests that the presence of pyrrolic-N sites favours the oxygen adsorption and the following electron transfer.

Another example of C-dots that only generate $^1O_2$ are the CQDs, still prepared from citric acid and 1,5-diaminenaphtalene via solvothermal synthesis, which absorb in the 200 – 350 nm range and do not form $O_2^{\bullet-}$ and $^{\bullet}OH$ [74].

Doping C-dots with heteroatoms besides N

Another experimental observation is that doping the C-dots with highly electronegative atoms, such as Cl, promotes the energy transfer to O_2 increasing the GQD activity as oxidant [75]. The energy transfer happens in the "classic" way from the excited triplet state of Cl doped GQDs to the ground-state oxygen. The same sample does not produce $O_2^{\bullet-}$ or $^{\bullet}OH$ under irradiation while if not illuminated behaves as radical scavenger (vide infra). A comparison with the undoped GQDs shows that the presence of Cl atoms increases three times the capability of forming $^1O_2$. It has been also observed that a higher content of Cl favours the formation of defects, in particular carboxylic and carbonyl groups (vide infra) that in GQDs have been associated to a higher ROS generation capability.

Enhanced $^1O_2$ generation has been also observed in red emissive carbon dots synthesised using methylene blue as carbon source and KH_2PO_4 to modify the graphenic structure adding P heteroatoms [76]. The P doped C-dots have a longer excited triplet lifetime with respect to reference dots prepared using only methylene blue and have a singlet oxygen quantum yield of 0.91. The long lifetime, 1.76 μs, which gives more time to interact with $^3O_2$, is considered the cause of the efficient $^1O_2$ generation.

The role of surface functional groups on ROS generation

Addressing an effective design of C-dots with ROS generation capability requires a fundamental understanding of the role of oxygen functional groups (OFGs) on the surface of carbon dots. OFGs play an active role in catalyzing several reactions, as they do in many carbon-based materials. Qu et al. [77,78] have carried out an in-depth investigation into the role of various OFGs on the surface of GQDs. They have identified three OFGs on the surface of GQDs, ketonic carbonyls (-C═O), hydroxyl (-C-OH) and carboxyl groups (O═C-O-) (Fig. 8). Each one of these groups has been correlated to a specific catalytic function: active sites for the decomposition of H_2O_2 and generation of hydroxyl radicals (-C═O), substrate binding sites (-C-OH) and inhibiting sites of the reaction (O═C-O-) [79]. A selective removal of these oxygen functional groups has allowed to identify the more active sites in the generation of ROS, upon irradiation with blue light (450 nm). The ketonic groups are the most effective in forming radical species. In general, a removal of the

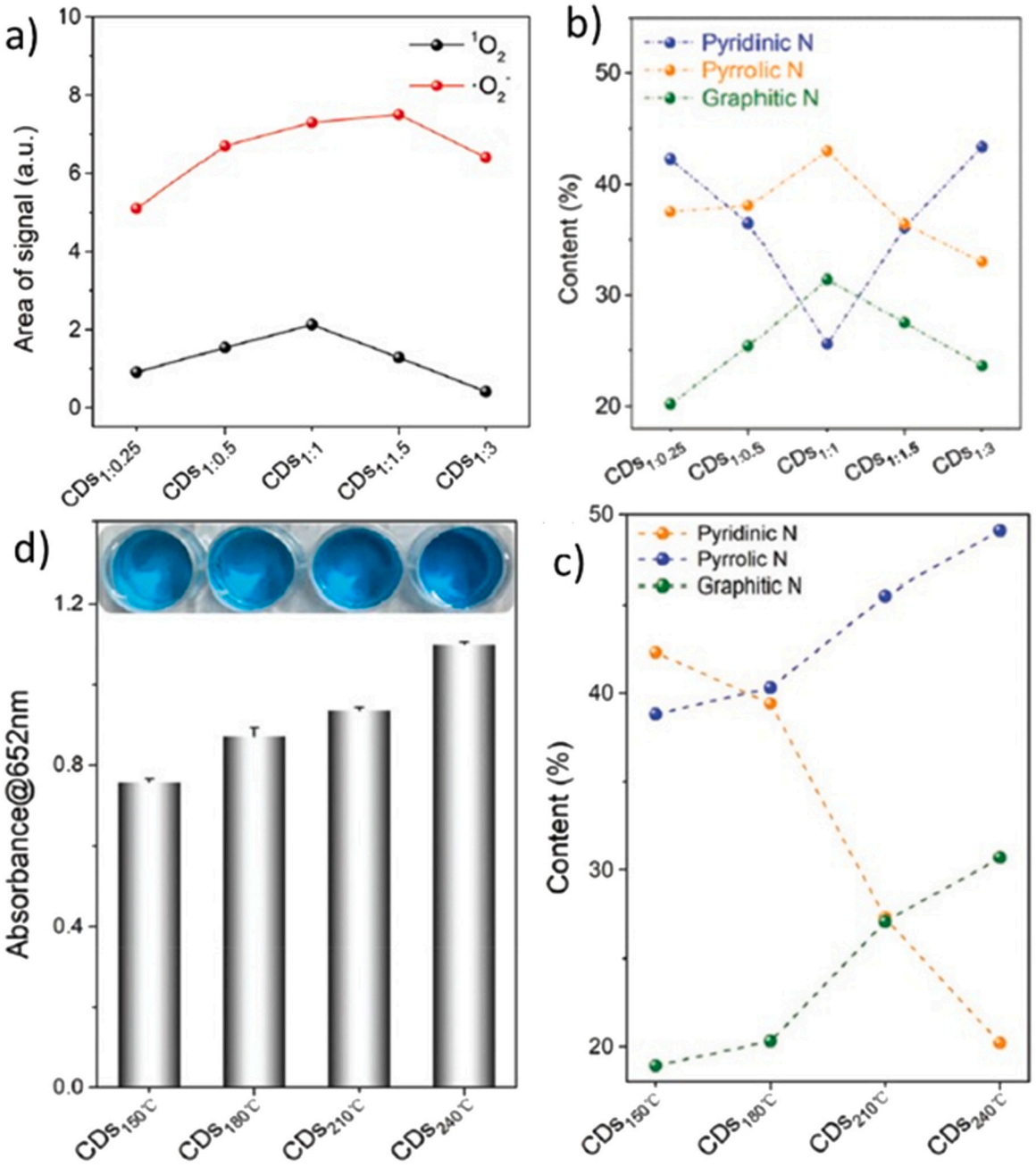

Fig. 7. a) Integrated EPR area of $^1O_2$ and $^{\cdot}O_2$ from five N-CDs prepared with different citric acid/ethylenediamine molar ratios. b) Changes in the content of the nitrogen doping types as a function of precursor (citric acid/ethylenediamine) molar ratios. c) Changes in the content of nitrogen doping types for CDs treated at different temperatures. d) Oxygen photosensitization of CDs treated at different temperatures in aqueous solution (10 μg mL^{-1}) under 365 nm LED irradiation.
Rearranged with permission from ref. [73].

Table 2
N content, fluorescence quantum yield (QY), and fluorescence lifetime of N-doped CDs synthesised using citric acid and ethylenediamine. 73.
Source:Redrawn with permission from ref.

Citric acid/ ethylenediamine (molar ratio)	Nitrogen content (%)	Fluorescence Fluorescence quantum yield (%)	properties Average lifetime (ns)
1: 0.25	5.4	20.38	8.4
1: 05	9.4	29.87	9.6
1: 1	10.7	50.14	13.4
1: 1.5	13.3	79.82	14.8
1: 3	16.0	57.23	14.9

oxygen functional groups, obtained by a chemical reduction of the GQDs, reduces the ROS production and, therefore, the photoinduced cytotoxic effect of the nanoparticles [80].

The preferential removal of OFGs can be used for the synthesis of GQDs enriched in one of the species. These findings have been used to design "nanozymes" that mimic the enzyme activity. The ability of C-dots of scavenging different types of radicals has been applied to extend their conceptual use as artificial nanozymes [81–83]. The importance of the OFGs as key elements to design the ROS activity has been confirmed by CQDs synthesised in autoclave using p-phenylenediamine and ethylenediamine as precursors [84]. The dots have a graphitic core, a spherical and dimension around 2.7 nm.

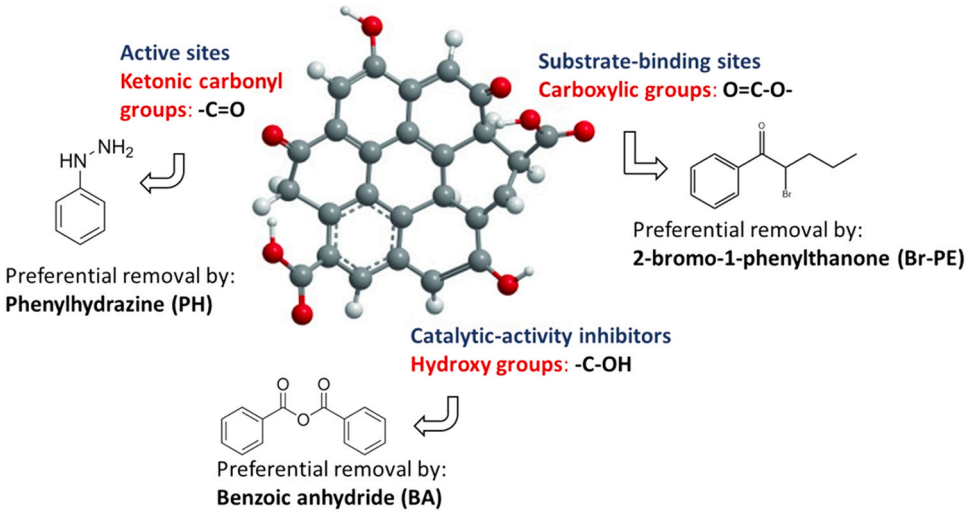

Fig. 8. Preferential removal of oxygen functional groups in GQDs to control the generation of ROS. See ref. 80.

Ultrasound generation of ROS

Another interesting experimental observation is that ROS can be generated by ultrasound irradiation of C-dots [85]. These dots find their field of application in sonodynamic therapy (SDT), which is based on the ROS emission upon low-intensity ultrasound stimulation [86]. The C-dots act as sonosensitizers to generate ROS that can induce tumour cell apoptosis.

One example of sonosensitizer C-dots for ROS generation are the dots prepared via a solvothermal route using copper(II) acetylacetonate ($Cu(acac)_2$), molybdenum dichloride dioxide (MoO_2Cl_2), and IR-780 iodide as precursors. The copper ions (Cu^+/Cu^{2+}) show a significant enhancement (about 160 times) of the reaction rate with respect to the iron redox couple (F^{2+}/Fe^{3+}) used in Fenton reactions, while molybdenum (Mo^{4+}/Mo^{6+}) promotes the formation of $O_2^{\bullet-}$. The as-prepared hybrid CDs exhibited near-infrared (NIR) emission and the capability of generating $^1O_2$ and $O_2^{\bullet-}$ when irradiated by ultrasounds. The structure of the dots has been described as a carbonaceous core formed by IR-780 and Mo and Cu oxide nanostructures. Interestingly, the presence of Mo, or Mo/Cu enhances only the generation of OH and $O_2^{\bullet-}$ species, while the C-dots prepared from IR-780 alone are better generators of $^1O_2$.

Another example is the C-dot synthesized by Shen and colleagues, which resulted in NIR-phosphorescent nanoparticles identified as bipolar quantum dots with both p- and n-type surface functionalization regions [87]. The p–n-CD material has been obtained via microwave synthesis at 200 °C using of a NIR-phosphorescent dye, indocyanine green, containing sulfonic (SO_3^-) acceptors and pyrrolic/graphitic N donators from branched polyethylenimine (Fig. 9). For comparison, p- and n-type C-dots have been prepared using only indocyanine green and 1,3,6-trinitropyrene in combination with branched polyethylenimine, respectively. The different syntheses produces C-dots whose surface is modified with SO_3^- acceptors (8.1 at%), pyrrolic N (7.3 at%), and graphitic N (2.5 at%) donators (p-n-C-dots), donators while the p-CDs, surface is rich of SO_3^- acceptors and that of n-CDs in pyrrolic and graphitic N donators. The various dots are characterized by different energy bands, with the p-n-CDs the narrowest one; they also exhibit the highest ultrasound stimulated ROS emission. The combination of long lifetime of the excited triplet state and the inhibition of the e^-–h^+ pair recombination given by the p–n junction has been considered at the ground of the efficient $^1O_2$ generation stimulated via ultrasounds.

Design of ROS emitting C-dots

The previous discussion and the reported experimental cases allow making some critical considerations about the generation of ROS from C-dots. The data, even if not exhaustive, show that several

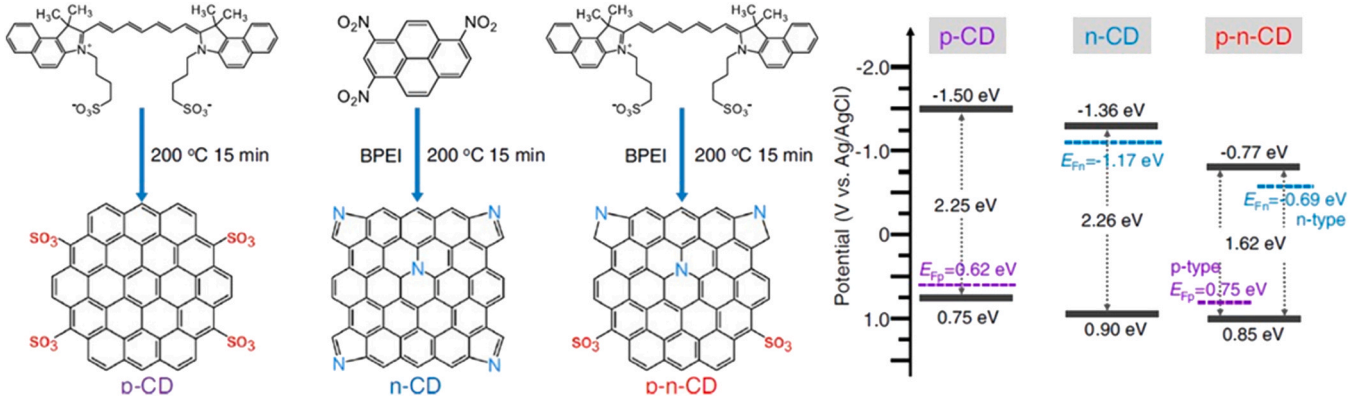

Fig. 9. Left. NIR infrared emitting C-dots prepared using indocyanine green (p-CDs), 1,3,6-trinitropyrene and branched polyethylenimine (BPEI) (n-CDs) and indocyanine green in combination with branched polyethylenimine (p-n-CDs). Right. Schematic illustration of the energy-band diagrams of the p-CDs, n-CDs, and p–n-CDs.
Rearranged with permission from ref. [87].

parameters affect the design of the carbon nanoparticles as ROS generators. It should also be recognized that some of the C-dots emit ROS under UV light stimulation, other when irradiated in the visible range. Applications for photodynamic therapy clearly require photostimulated ROS emission by visible and near-infrared light. This is a design parameter that has to be carefully considered, some C-dots appear to be excellent ROS generators but only upon stimulation by UV light, which is a limitation for most of the potential applications. It should be also noticed that while the C-dots can generate singlet oxygen not always this is accompanied by the capability of generating $^{\bullet}OH$ and $O_2^{\bullet-}$. The radical species and the singlet oxygen are formed via two different mechanisms, as we have seen, and if a specific C-dot is able to transfer energy to molecular oxygen in the ground state, not necessarily is capable of electronic transfer. Another important observation is that the ROS generation property is a combination of several factors, a summary of the most important is the following:

1. *Lifetime in the triplet excited state*. Higher lifetimes favour in principle the energy transfer to $^3O_2$, however, the experimental data show also that other parameters are more effective to induce ROS generation.
2. ΔE_{ST}. A smaller singlet-triplet energy gap, ΔE_{ST}, favours intersystem crossing and ROS generation. This property can be tuned via doping with specific N-sites.
3. *Oxygen absorption.* A better absorption capability of $^3O_2$ by the C-dots promotes the energy and electron transfer for ROS generation via Type I and Type II photoreactions.
4. *Oxygen functional groups.* The ROS generation is also dependent on the presence on the surface different types of oxygen functional groups. Ketonic carbonyl groups promote the generation of hydroxy radicals.
5. *Doping the C-dots with heteroatoms*. Electronegative atoms, such as Cl, promotes the energy transfer to O_2.

The previous summary can be used to address the proper design of C-dots with the capability of generating ROS (Fig. 10).

It shows what are the main parameters affecting the ROS generation capability from C-dots, but much care has to be done in a comparative evaluation of the performances, because only few works report the singlet oxygen quantum yield, and this is measured using different methods with a potentially high experimental error. It has also to be considered that other factors are not in general considered, for instance, the effect of the dimension and shape is seldom evaluated. Basically, every synthesis produces C-dots with a variety of structures and properties, and even small changes give different nanomaterials.

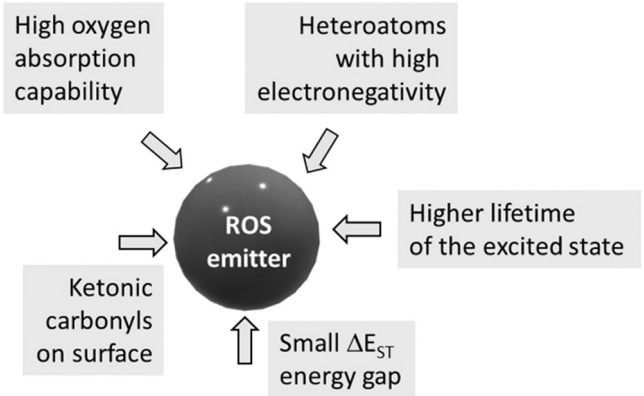

Fig. 10. A schematic description of the main factors affecting the capability of a C-dot to generate ROS.

Radical scavenging properties

Besides carbon dots, carbon-based nanomaterials include a wide variety of nanostructures such as fullerenes, nanodiamonds, nanotubes, and graphene. These materials share with C-dots the capability to act as radical scavengers under some conditions. Fullerenes and fullerene derivatives are well known for their ability to scavenge free radicals through the combination of two separate mechanisms: electronic transfer and adduct formation [88,89]. Carbon nanotubes [90,91] and functionalized graphene [92,93] have also shown a significant radical scavenging activity.

In general, different mechanisms are responsible for radical scavenging, alone or in synergy:

1. Hydrogen transfer from surface functional groups.
2. *Electron transfer mechanism* (ETM). ETM can be explained and visualized through a donator acceptor map (DAM) [94] that indicates whether a molecule is a good electron donor or acceptor [95].
3. *Formation of radical adducts at sp^2 carbon sites.* The presence of sp^2 rich domains favours the formation of adducts with the radical species [96]. They delocalize the electrons in the conjugated graphene-like regions and eliminate the radicals by forming a second adduct.

Antioxidants are divided into enzymatic, such as superoxide dismutase, catalase, peroxidase, ascorbate peroxidase, etc., and nonenzymatic as polyphenol, phenolic acids, flavonoids and ascorbic acid [97]. C-dots fall into the nonenzymatic radical scavengers.

C-dots show a large variability regarding their radical scavenging activity that changes with composition and structure. They exhibit also performances that are depending on the type of radicals; for this reason, the section dedicated to the radical scavenging activity has been discussed considering the response as a function of the different radicals and the peculiar class of C-dots.

Scavengers of reactive nitrogen species

Nitrogen reactive species scavenging by carbon nanodots (CNDs)

Radical scavenging of nitrogen reactive species has been observed in different carbon nanomaterials [98,99]. In particular, C-dots have an experimental reported antiradical activity towards reactive nitrogen species (RNS), $NO^{\cdot}$ and $NO_2^{\cdot}$, which can interfere with the cellular activity. The scavenging activity is evaluated by measuring the radical content in solutions containing the dots with respect to a control without. The standard molecule employed for this purpose is 1,1-Diphenyl-2-picrylhydrazyl radical ($DPPH^{\bullet}$), (Fig. 11) a stable, nitrogen-centered free radical [100] whose nitrogen has two lone-pair electrons surrounded by three benzene rings. $DPPH^{\bullet}$, because of its electronic configuration, easily accepts an $H^{\bullet}$ radical to form the stable diamagnetic DPPH-H complex.

$DPPH^{\bullet}$ is employed to test the scavenging properties by measuring the attenuation in the Electronic Spin Resonance (ESR) signal generated by a free radical in presence of the dots. The scavenging works via donation of a hydrogen atom or even electron transfer.

Besides ESR is also possible to use a simpler detection method based on UV-Vis spectroscopy and $DPPH^{\bullet}$. $DPPH^{\bullet}$, in fact, in a methanolic solution absorbs in the visible region with a maximum peaking around 517 nm. The solution loses its coloration with the increase in concentration of antioxidant C-dots; the decrease of the absorption band allows evaluating the scavenging activity [101].

The method has been widely applied for the C-dots and several examples have been reported for samples prepared from natural products. For instance, S and N doped C-dots prepared via hydrothermal synthesis at 200 °C using garlic as natural precursor have a scavenging activity towards RNS [102]. The authors, however, do not

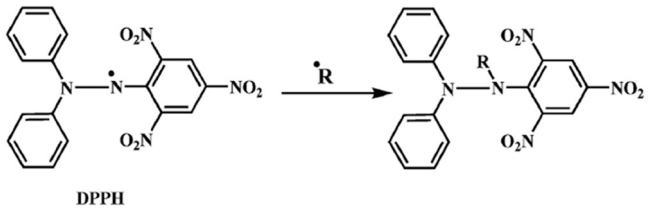

Fig. 11. 1,1-Diphenyl-2-picrylhydrazyl radical (DPPH$^{\bullet}$) and its reaction with R radicals (H$^{\bullet}$, alkyl radicals, etc.).

give the composition of the garlic neither specify the type and origin making reproducibility of the process highly questionable while also the mechanism of action is not described in detail. The C-dots are able to quench the RNS within a couple of minutes showing also a dose dependence (Fig. 12).

Several works have been dedicated to directly synthesizing C-dots from natural products; however, most of these works lack experimental details that are critical for reproducibility and characterization of the material. While the scavenging properties are generally well described, a thorough analysis and description of the mechanism is rarely reported or does not have the support of specific experiments. Scavenging activity to RNS has been reported for C-dots synthesised from: date melassa [103], Thymus vulgaris [104], natural extracts such as lutein [105], coriander leaves [106], green tea leaves [107] and grape pomasse [107], to cite some.

A comparison of these works shows that, in general, the emission is excitation dependent and confined in the blue. A strong dependence on the concentration is also observed. A comparison of EC50 values (half maximal effective concentration) (Table 3), which express the amount of antioxidant required to inhibit radicals by 50%, reveals that C-dots generally underperform when compared to standard antioxidants used as references, such as Ascorbic acid or Vitamin E. This is also related to the inherent difficulty of the synthesis; achieving precise control of the surface that governs the antioxidant properties is a hard task. In general, the published works do not yet allow for a thorough understanding of the process. Table 4.

An explanation for the possible mechanism of radical scavenging is connected to hydrogen transfer from C-dot surface groups to DPPH$^{\cdot}$. The presence of carboxyls (-COOH), hydroxyls (-OH) and amino (-NH_2, -NH) groups allows the hydrogen transfer and the reduction of DPPH$^{\cdot}$ to DPPH-H. The unpaired electrons on the C-dot surface can be delocalized by resonance within the aromatic domains or through chemical bond rearrangement (Fig. 13). Blue fluorescence of C-dots, on the other hand, is quenched by an electron transfer mechanism in which nitroxide radicals act as electron acceptors.

Nitrogen reactive species scavenging by graphene quantum dots

Graphene quantum dots (GQDs) have also been exploited as potential radical scavenger of nitrogen reactive species [108]. The presence of sp^2 bonds and unpaired electrons should favour the radical scavenging activity and this has been tested by ESR (Fig. 14). Even in this class of C-dots there is a large variability in the RNS scavenging performances that depend on the synthesis method. GQDs, prepared from graphite via acidic exfoliation and fragmentation, quench the RNS even if the EC50 is around 150 μg mL^{-1}.

A significant improvement of the radical scavenging activity is observed in C-dots doped with non-metallic heteroatoms such as Mn and P [109]. The doped C-dots show an EC50 value of 6.55 μg mL^{-1}, which is close to that one measured for the standard ascorbic acid, 4.03 μg mL^{-1}. Still in the best case the C-dots appear to underperform in comparison to standard RNS scavengers. Even C-dots preparing using ascorbic acid do not show a better performance in terms of RNS scavenging activity [110]. C-dots synthesised in hydrothermal conditions from resorcinol and ascorbic acid have a EC50 around 50 μg mL^{-1}. Similar values, around 40 μg mL^{-1}, have been obtained for C-dots doped with Selenium [111].

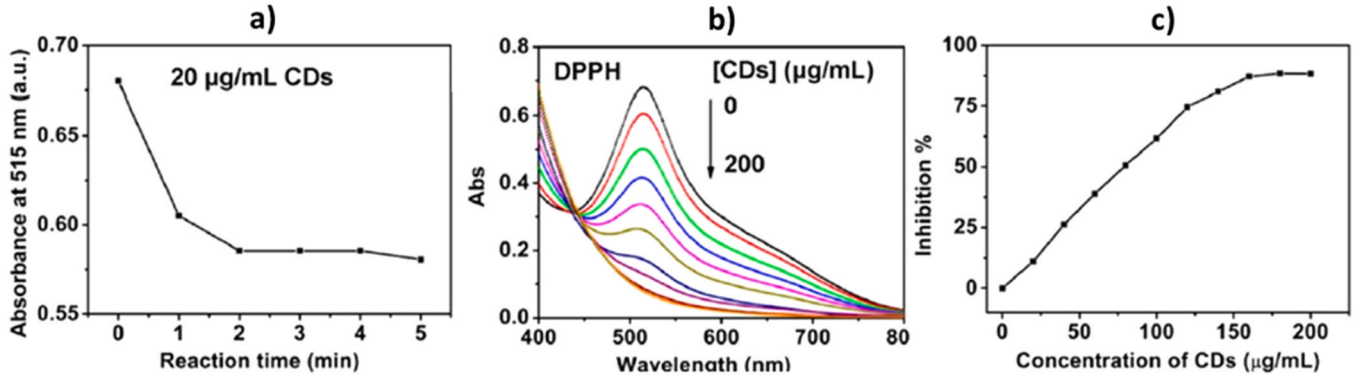

Fig. 12. Scavenging of DPPH radical. (a) Scavenging of DPPH radicals as a function of time in the presence of 20 μg mL^{-1} C-dots. (b) Absorbance titration spectra of DPPH upon gradual addition of C-dots from 0 to 200 μg mL^{-1}. Scavenging of DPPH$^{\cdot}$ radicals as a function of (c) Scavenging of DPPH$^{\cdot}$ radicals as a function of C-dots concentration. Reproduced with permission from ref. 102.

Table 3
Calculation of the singlet excited (S_1) – triplet excited (T_1) energy gap (in eV and kJ mol^{-1}), and adsorption energy of oxygen (E_{ads} in eV) in graphitic-N, pyridinic-N and pyrene-N structures (inset in the table), using a coronene or pyrene model. Data from ref. 73.

	Graphitic-N		Pyridinic-N		Pyrene-N	
Coronene model	$S_1 \rightarrow T_1$ 0.524 eV 50.5 kJ mol^{-1} E_{ads} = −1.4768 eV		$S_1 \rightarrow T_1$ 0.649 eV 62.6 kJ mol^{-1} E_{ads} = −1.2690 eV		$S_1 \rightarrow T_1$ 0.794 eV 76.6 kJ mol^{-1} E_{ads} = 0.1899 eV	
Pyrene model	$S_1 \rightarrow T_1$ 0.598 eV 57.7 kJ mol^{-1} E_{ads} = −1.3634 eV		$S_1 \rightarrow T_1$ 1.051 eV 101.4 kJ mol^{-1} E_{ads} = −1.1342 eV		$S_1 \rightarrow T_1$ 1.175 eV 113.4 kJ mol^{-1} E_{ads} = 0.0792 eV	

Table 4
Nitrogen reactive species scavenging activity by carbon nanodots.

Precursor	Synthesis	Structure	Dimension	Emission / EC (50)	Reference
Natural garlic (composition and origin unknown)	Hydrothermal – 200 °C	Graphitic. d_{002} = 0.35 nm graphitic plane. N and S doped	10.7 average size (by TEM)	Blue (λ_{em} = 440 nm) EC(50) = 80 μg mL^{-1}	[92]
Date melassa (composition and origin unknown)	Hydrothermal – 200 °C	Graphitic + C8 (perfluorooctanoic acid)	5.7 average size (by TEM)	Blue (λ_{em} = 480 nm) EC(50) = 40 μg mL^{-1}	[93]
Lutein (natural plant extract) + ethylenediamine	Hydrothermal – 140 °C	Not specified	40 nm average size (by LS)	Blue (λ_{em} = 460 nm) -	[95]
Thymus vulgaris L. (composition and origin unknown)	Hydrothermal – 200 °C	Not specified	8 nm average size (by TEM)	Blue (λ_{em} = 420 nm) EC(50) = 23 μg mL^{-1}	[90]
Green tea leaves (commercial company)	Carbonization 200 °C	Amorphous + graphite. Lattice space 0.19.	4 nm average size (by TEM)	Blue (λ_{em} = 430 nm) EC(50) = 50 μg mL^{-1}	[97]
Grape pomace	Hydrothermal – 180 °C Oven 180 °C	Amorphous	3.5 nm average size (by TEM)	Blue (λ_{em} = 430 nm) Blue (λ_{em} = 440 nm) EC(50) = 15 μg mL^{-1}	[97]
Coriander leaves (composition and origin unknown)	Hydrothermal – 240 °C	Amorphous	2.4 nm average size (by TEM)	Blue (λ_{em} = 400–510 nm) EC(50) = 75 μg mL^{-1}	[96]
Precursor	**Synthesis**	**Structure**	**Dimension**	**Emission**	**Reference**
Glutathione + citric acid	Hydrothermal – 180 °C	Amorphous	6 nm (by TEM)	Blue (λ_{em} = 418 nm) EC(50) = 175 μg mL^{-1}	[107]
p-phenylenediamine Phosporic acid $Mn(OAC)_2$	Microwave	Crystalline, d_{001} = 0.21 and 0.25 nm	6.5 nm (by LS)	Red (λ_{em} = 600 nm) EC(50) = 6.55 μg mL^{-1}	[99]
Resorcinol + Ascorbic acid	Hydrothermal 200 °C	Crystalline, d_{001} = 0.21	~ 3 nm (by TEM)	Blue (λ_{em} = 440 nm) EC(50) ~ 50 μg mL^{-1}	[100]
Selenocystine	Internal circulation rotating packed bed	Amorphous	2 nm (by TEM)	Blue (λ_{em} = 490 nm) EC(50) ~ 40 μg mL^{-1}	[113]
Graphite – γ irradiation N and/or S doping	Graphite electrode	Crystalline, d_{1120} = 0.21 nm	5.8–21 nm 7.0–17.6 nm (by TEM)	- EC50 = 129 μg mL^{-1}	[102]
Graphite	Fragmentation of graphite by acids (GQDs)	Not reported	3–6 nm (by TEM)	Not reported	[98]
Carbon black (GQDv) Pyrene (GQDp) Glucose (GQDg)	Oxidative exfoliation Hydrothermal Hydrothermal (GQDs)	graphene	2.8 (lat) – 1.0 (h) nm 2.7 (lat) – 1.5 (h) nm 2.2 (lat) – 2.2 (h) nm	530 nm (GQDv) 490 nm (GQDp) 395 nm (GQDg)	[106]
Branched polyethylenimine cysteine phosphoric acid crystals N, P, S doping	Hydrothermal – 180 °C	Not reported	2.2–5.6 nm by TEM	- EC(50) = 197 μg mL^{-1}	[103]
Sucralose Cl doping(GQDs)	Electrochemical method	Crystalline, d_{1120} = 0.24 nm	~ 2 nm by TEM (deduced by image)	430 nm - Dual property Oxidant - antioxidant	[65]

The effect of doping on RNS has been also evaluated comparing GQDs, N-doped GQDs and GQDs doped with dual heteroatoms, S and N [112]. Only the sample doped with N shows a detectable RNS activity, but still much lower in comparison to Vitamin C, with and EC50 = 129 μg mL^{-1}. Doping with dual heteroatoms, N and S, quenches instead the RNS scavenging activity. Multiple doping with N, S and P atoms does not also improve the RNS scavenging (EC50 = 197 μg mL^{-1}) [113].

The anti-oxidant properties of graphene, which have been found to be dependent on its structure, provide some insights about the mechanism that is responsible for scavenging. The radical scavenging activity of graphene oxide (GO), reduced graphene oxide (rGO), and few-layer graphene (FLG) against RNS, changes according to the structure [114]. Fig. 15a shows the RNS antioxidant response of GO, with respect to some reference molecules included the fullerene derivative pyrrolidine (FDP) that is a commercially available and water-soluble fullerene derivative with anti-oxidant properties. GO shows only a moderate antioxidant activity with around 15% radical reduction. Acid ascorbic and fullerene derivatives have, instead, a much more effective radical scavenging activity with around 60% reduction (Fig. 15b).

GO shows, therefore, a weak activity toward DPPH· in comparison to reference antioxidants and FDP. Because scavenging of DPPH· generally, occurs via hydrogen donation, the weak GO response indicates that is a poor H donor. This is not very surprising because of the relatively high hydroxy content in GO. The hydrogen transfer from a generic molecule M, which is a hydrogen donor, goes through:

$$MH + R^{\cdot} \rightarrow RH + M^{\cdot},$$

where the new radical M· is enough stable to stop the free-radical chain reaction. In GO, however, is present a low number of phenolic OH groups. In fact, several antioxidants are phenolic compounds, whose radicals are stabilized by resonance structures. In this configuration the unpaired electrons can reside on the oxygen atom, or on ortho or para carbons on the adjacent aromatic ring. In GO most of the hydroxyls should be located out-of-plane with respect to the

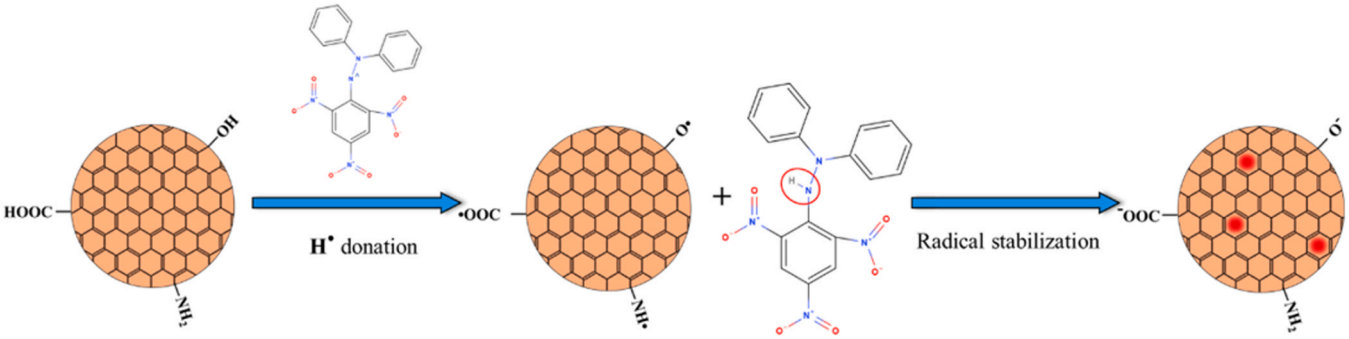

Fig. 13. Mechanism of DPPH· reduction by antioxidant C-dots in aqueous media.

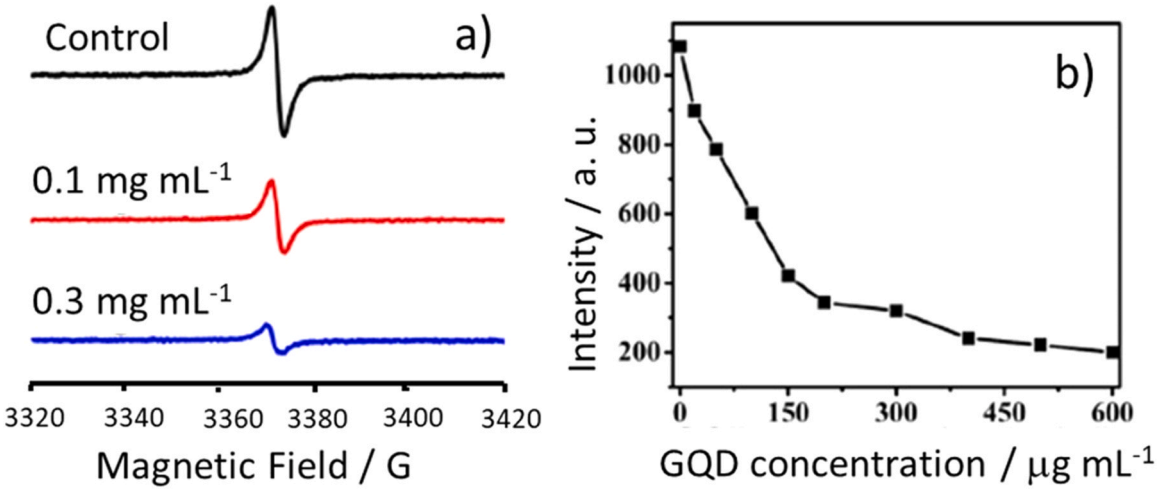

Fig. 14. a) ESR spectra of DPPH• of samples containing 0.1 mM DPPH•, 10 mM PBS buffer (pH 7.27), and different concentrations of GQDs. Data were recorded 5 min after incubation. (b) Effect of GQD concentration on their DPPH•-scavenging activity.
Reproduced with permission from ref. [108].

basal sites. The oxidation of the C═C double bond is reflected in the formation of sp^3 sites that lack of the adjacent conjugated structure that stabilizes the radical resonant electron. In GO, the phenolic OH groups are expected to be found only at the structure edges and not in the basal plan, reducing, therefore, the proton donor capability of the graphene oxide structure.

A direct demonstration of the primary role played by phenolic groups as active sites for proton transfer has been obtained by reducing a CQD that after the synthesis is rich in OFGs (C═O, C-OH, and COOH). The reduction by $NaBH_4$ succeeds in converting C═O to C-OH creating phenol-like groups in the dot [115]. Even though the carboxyl groups and the total oxygen are unaffected by the

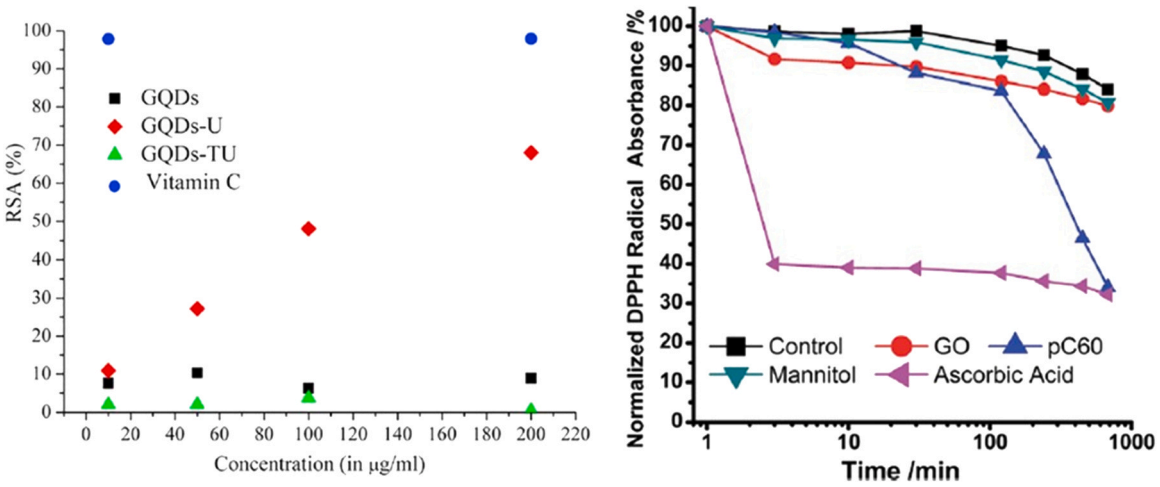

Fig. 15. a) Radical scavenging activity (RSA) vs.concentration calculated from the UV-Vis spectra of DPPH. andmixtures of DPPH. with different concentrations of GQDs,GQDs-U (GQDs prepared with urea and GQDs-TU (GQDs prepared with urea andthiourea). Vitamin C was used as a standard. Reproduced with permission fromref. 113. b). Interaction of grapheneoxide and reference antioxidants (100 pm) with the model stable free radicals DPPH
Reproduced with permission from ref. [115]

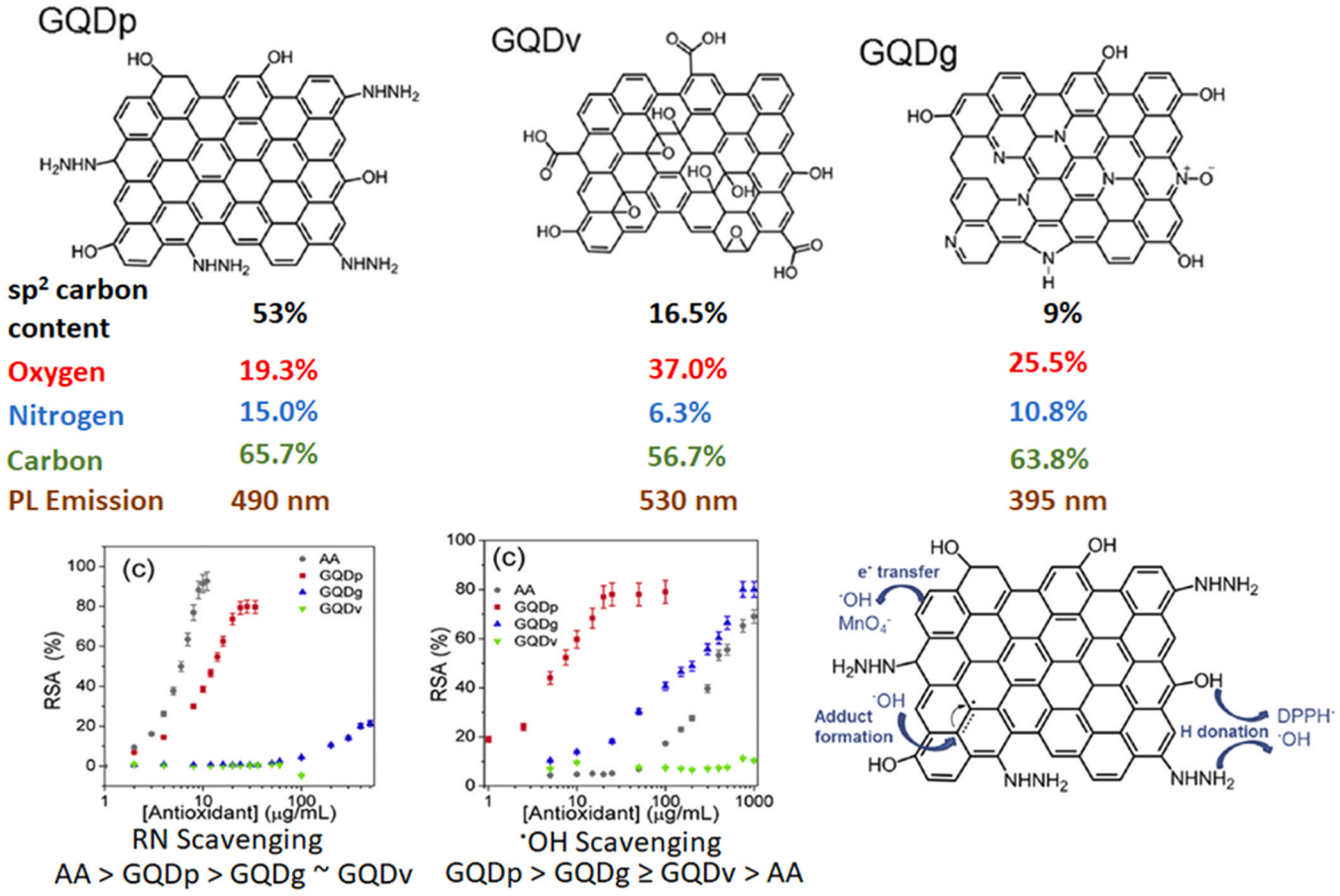

Fig. 16. GQDs structure identified by XPS (top); Bottom left, DPPH· scavenging assay, radical scavenging activity (RSA) vs. antioxidant concentration; bottom middle, Hydroxyl radical scavenging assay, RSA vs. antioxidant concentration; Bottom right, mechanism for antioxidant activity of GQD.
Rearranged with permission from ref. [116].

reduction, around 75% of the OFGs change to C-OH during the process. In contrast to GQDs still containing carboxylic species, the DPPH· test revealed that substantial amounts of phenol-like groups improve the radical scavenging action. Theoretical calculations have also revealed the importance of adjacent oxygenated groups to modulate the OH bond dissociation energy of phenol-like groups. Furthermore, the proton donor activity of the phenol-like species can be reduced by the presence of close carbonyl groups. This implies that, as a general strategy, effective antioxidant CQDs should be rich in phenolic groups while avoiding or limiting the presence of carbonyl groups.

The main issue in evaluating C-dot performances as radical scavengers is the experimental limitations in defining the exact composition in terms of structure and surface. GQDs have an inherent advantage in this regard because their structure is entirely graphenic, even if surface and edge groups play an important role. In GQDs, a more effective structure-property comparative evaluation is possible. This is exactly what has been done by Ruiz et al. who compared the antioxidant activity of GQDs prepared in different ways and whose structure has been carefully characterized [116]. Three different types if GQDs have been prepared, one from oxidative exfoliation of carbon black nanoparticles (GQDv), another by hydrothermal treatment (HT) of glucose in ammonia (GQDg) and a third one by HT treatment of pyrene (GQDp). The main findings of the work are resumed in the Fig. 16.

The three types of GQDs are characterized by different contents of sp^2 carbons, with a much higher content in GQDp. The various compositions are reflected in a different radical scavenging performance. GQDp shows a much better capability of radical scavenging toward RNS than hydroxyl radicals. It is interesting also to observe that all the systems are underperforming as RNS scavengers with respect to the standard antioxidant, ascorbic acid (AA), while are overperforming in the case of ·OH. The better scavenging activity of GQDp for nitrogen reactive species is correlated to the presence of functional groups at the edge sites, -OH and -$NHNH_2$, combined with an extended network of sp^2 carbon atoms. The functional groups act as hydrogen donors, while the graphenic structure stabilizes and delocalizes the free electrons. This property is critical, because comparing the scavenging activity with GQDv, which are characterized by a large number of OH groups, and GQDg that have pyridinic nitrogen, the combination between high content of sp^2 bonds and functional groups is fundamental.

In the case of OH scavenging the formation of radical adducts at sp^2 C sites is the main scavenging mechanism. The higher scavenging capability of GQDp can be attributed to their larger sp^2 C domains that are the main ·OH scavengers. They result more effective than functional groups containing oxygen as shown by the studies on graphene derivatives previously discussed [114]. On the other hand, a ·OH scavenging activity is also shown by GQDg that have a lower sp^2 C content because the high N doping level favours the formation of radical adducts and the electron transfer. The highly oxidized GQDv, show instead almost no radical scavenging capability both for RNS and ·OH. This experiment gives a good indication how C-dots as radical scavengers should be designed. The combined presence of an extended graphenic structure with sp^2 bonds and edge groups that are proton donors favours GQDs as radical scavengers with respect to CNDs.

Another experiment that can also give some indication about the design of RNS scavenger carbon dots has been reported by Li et al.,

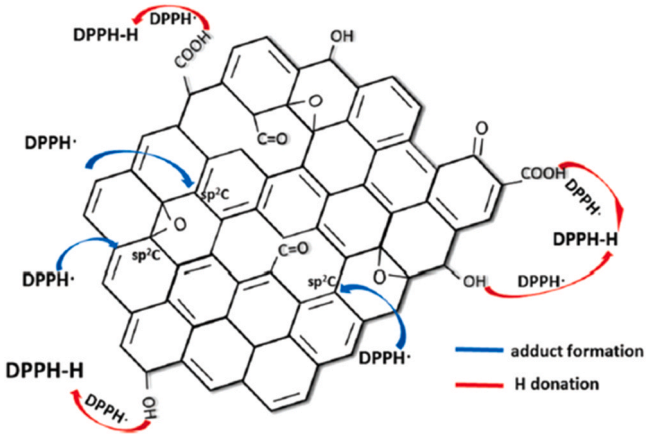

Fig. 17. Proposed mechanism for the reaction of GQDs with DPPH. Reproduced with permission from ref. [117].

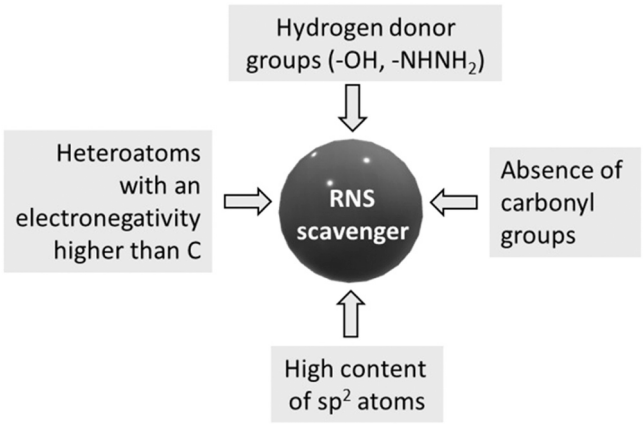

Fig. 18. A schematic description of the main factors affecting the capability of a GQD to be a radical scavenger of RNS.

who studied how the oxygen functional groups in GQDs affect the antioxidant activity [117]. GQDs with decreasing amount of O, obtained by a controlled reduction with a solution of sodium borohydride, also show a reduction in the scavenging activity to DPPH· that follows a similar trend. This reduction has also been associated with the change in the surface oxygen groups that have different antioxidant activities for DPPH·; in particular, C-OH and C=O groups are more active than C-O-C. The data indicate that the combined properties of being a hydrogen donor together with favouring the formation of adducts promote the antioxidant activity (Fig. 17).

Another important effect, with an electronegativity higher than carbon. The presence of such heteroatoms increases the sp^3 sites and the unbalanced distribution of the electronic charge within the hexagonal carbon rings, which in turn that on turn facilitates the electronic interaction between the dots and the radicals. An example is doping of GQDs with Cl, which as a higher electronegativity with respect to carbon, 3.16 (Cl) and 2.55 (C) [75]. Composition analysis performed on the Cl doped samples by XPS immediately after the reaction with DPPH· shows the presence of nitrogen, indicating the formation of adducts on the sample surface. XPS also shows that most of the C-O bonds reduce while C-Cl bonds disappear, showing that the reactive centers for RNS scavenging are oxygen and chlorine. The GQDs with the highest content of Cl, have a better electronic interaction between with DPPH• and the highest scavenging capability.

Another question to address, which has still to be fully investigated, is if using as precursor a molecular compound with a strong antioxidant activity is possible also to obtain C-dots that reflect such property [118]. The few results about seem to indicate that does not exist such direct relationship because during the C-dot processing, which generally involves the use of high temperatures and chemical reactions in uncontrolled conditions, the molecules can undergo to a significant transformation. It is a better strategy to focus on understanding which are the critical parameters that affect the radical scavenging activity and designing the synthesis according to.

To resume the previous discussion some indications how to design a GQD which is an effective RNS scavenger, are schematically shown in the Fig. 18.

Scavenging of hydroxyl radicals (·OH)

C-dots have shown the capability to scavenge different types of radicals, such as hydroxyl and superionic radicals (vide infra). Hydroxyl radicals are highly oxidising species that can quickly degrade several organic molecules; oxidative damage can be induced on DNA, lipids and proteins [119]. ·OH are one of the main sources of oxidative stress in biological systems.

To test the C-dot scavenging activity, the ability of the particles to reduce the hydroxyl radicals created on purpose in solution has been measured. The main method uses the in situ generation of hydroxyl radicals by Fenton reaction based on the oxidation of iron(II) by H_2O_2 ($Fe^{2+} + H_2O \rightarrow {\cdot}OH + OH^- + Fe^{3+}$). Hydroxyl radicals are also generated in solution upon dispersion of TiO_2 nanoparticles and irradiation with UV light [108]. 5,5-Dimethyl-1-pyrroline N-oxide (DMPO) that forms the spin adduct DMPO/OH·, is used to trap the hydroxyl radicals and quantify the scavenging ability of C-dots by ESR spectra. Another optical method is based on evaluating the attenuation in presence of the C-dots of a dye bleaching activated by hydroxyl radicals [116] or using the 3,3′,5–5′-tetramethylbenzidine (TMB) radical assay [109].

Scavenging of hydroxyl radicals has been reported for several C-dots of different compositions and structures. However, a critical comparison is difficult due to the variety of testing procedures and the significant variability in C-dot compositions described in the literature. The best way to measure how well a radical scavenger works is to compare the experimental results to a standard antioxidative molecule. The performances of GQD as ·OH scavengers, just previously discussed, show for the GQDs sample an EC50 of 7.5 μg mL^{-1}. This value indicates that the GQDs have a radical scavenging activity higher than the reference ascorbic acid [116]. These performances are better than those reported for CNDs obtained from natural products that have a reduced scavenging activity for hydroxyls radicals [102,103]. CQDs doped with P^{3+} and Mn^{2+} have instead a noticeable antioxidant activity with an EC50 = 6.44 μg mL^{-1} that is almost comparable to the reference ascorbic acid (EC50 = 2.17 μg mL^{-1}). An improvement in the OH· scavenging efficiency has been observed in P doped GQDs with respect to the undoped samples [120]. On the other hand doping with S, N and P atoms give an EC50 = 396 μg mL^{-1}, which supports the fact that the C-dots without a rational design, even if they show some radical activity, cannot be compared to a single molecule antioxidant that has a well-defined structure and composition [113].

It should be noticed that a comparison of the E50 for ascorbic acid reported by the different research groups shows a quite large variability because standard experimental conditions cannot be applied. A correct comparison can be done only using the same set of experimental data of the single research group.

The antioxidant activity of Se [121] has been exploited by several research groups to prepare C-dots with free radical scavenging capability [122–125]. The antioxidant activity has been tested in vitro [122,123] and in vivo [124,125]. The samples have been prepared by hydrothermal treatment at 60 °C using selenocystine as the

precursor for doping the carbon structure with selenium. The Se-dots are CQDs formed by a combined amorphous-crystalline structure with an interlayer spacing similar to bulk graphite. The different reports show free radicals activity to ·OH, and low toxicity even if the performances have not been compared with standard antioxidants. Interestingly, Chen and coworkers [123] have simulated the scavenging activity of Se-doped C-dots using two models of bi-layered structures composed of four six-membered carbon rings, containing a substitutional amount of Se atom. The carbon regions are formed by an equally distributed combination of sp^2 and sp^3 carbon atoms. The models consider Se doped sp^3-C and Se doped sp^2-C structures (path I and path II in Fig. 19) as radical scavengers. The process in path II has a lower potential barrier and is not likely to scavenge the hydroxyl radicals.

The Se doped sites are electron donors and become radical scavengers by transferring electrons to the radicals, while the hole takes part in the transformation of the adducts. The modelling and the experiments with Se doped C-dots well support the importance of sp^2 sites for radical scavenging of C-dots (vide supra). The model considers only a small structure of two graphenic layers doped with selenium. The real case, however, must still take into account the formation on the surface and edges of functional species that nevertheless play an important role in radical reduction.

A comparison with the graphene capability of removing the hydroxyl radicals can give some additional indications about the scavenging mechanism [93]. Fig. 20**a** shows how different graphene materials, GO, rGO and FLG (vide supra) work as radical scavengers in comparison to other antioxidants (mannitol, pC_{60} and ascorbic acid). The antioxidant activity of graphene follows the order: FLG > rGO > GO. The difference is explained on the ground of the extension of the sp^2 domains in the graphene structures. The sp^2 sites, in fact, are considered to be the primary scavenging sites that work via adduct formation or electron transfer (Fig. 20**b**).

Scavenging of superoxide radical anions ($O_2^{\cdot-}$)

The C-dots have been tested also as scavengers of superoxide radical anions ($O_2^{\cdot-}$) that form via one-electron reduction of oxygen molecules, O_2. An excess of $O_2^{\cdot-}$ can accelerate the aging processes and the proliferation of cancer cells, via lipid peroxidation. In biological systems $O_2^{\cdot-}$ is scavenged by antioxidant enzymes through disproportionation to H_2O_2 and O_2.

ESR with a proper spin trap, such as 5-tert-Butoxycarbonyl-5-methyl-1-pyrroline-N-oxide (BMPO), is generally applied to test the scavenging ability of C-dots while enzymatic xanthin-xanthine oxidase is used to generate the $O_2^{\cdot-}$ anions in solution [126].

The reports about the radical antioxidant activity for the C-dots are lower in comparison to RNS and hydroxyl, and in general they do not perform well to reduce the $O_2^{\cdot-}$, with some few exceptions. Also, in the case of graphene materials, GO has shown only a modest scavenging activity against superoxide in comparison to ascorbic acid and pC_{60} [93].

Scavenging activity of C-dots has been reported for P^{3+} and Mn^{2+} with a better performance in terms of EC50 than for the ·OH radicals [109]. Strong scavenging toward superoxide radical anions has also been demonstrated for GQDs, even if the data have not been compared to a standard [108].

The formation of $O_2^{\cdot-}$ depend on the electron transfer ability of the system, as we have previously discussed for the generation of singlet oxygen. In this case the capability of the system to adsorb the oxygen molecules is also very important and a proper design of the system is necessary.

Dual oxidant-antioxidant nature of carbon dots

In the previous paragraphs, we have described how a dual nature characterizes C-dots, i.e., they can be either emitter of radical species acting as oxidants or scavengers of radical species working as antioxidants [127]. These properties are not surprising because they are exhibited by many carbon-based nanostructures such as fullerenes. Indeed, C_{60} is one of the most efficient sensitizers for singlet oxygen generation but is also, at the same time, an effective radical scavenger. These molecules, therefore, become a photosensitizer when excited by light. The triplet state enables an energy intersystem crossing with molecular oxygen and generation of ROS and singlet oxygen.

On the other hand, if they are not stimulated by light, they can function as very efficient antioxidants and again C_{60} is a nice example. In C-dots, because of the high variability in the possible structure the property of being oxidizing and antioxidant (OxAntiOx) is more elusive to define a priori.

Experimental data need also to be evaluated with care because the measures of the scavenging or oxidizing activity are generally done using different systems, such as optical probes or ESR, and a direct comparison is difficult.

An example of antioxidant-prooxidant C-dot is the system obtained by laser ablation of graphite and surface passivated with poly (propionylethyleneimine-coethyleneimine) or PEG_{1500} [128]. Upon

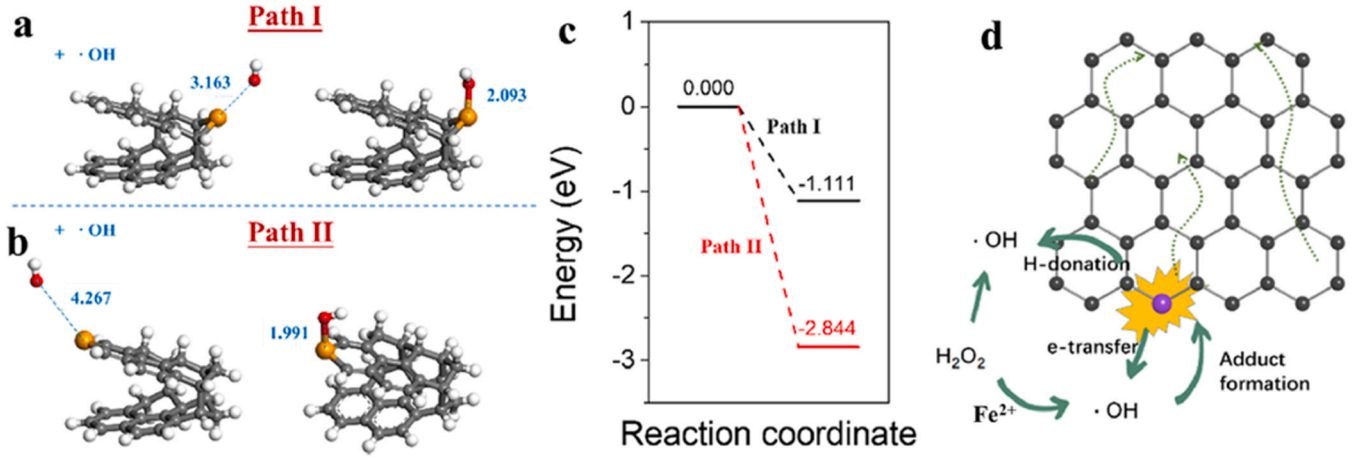

Fig. 19. Optimized processes of ˙OH combined on (a) Se doped sp^3-C and (b) Se doped sp^2-C. The gray, orange, red, and white spheres refer to C, Se, O, and H atoms, respectively; (c) combination energy profile at different coordinates of the ˙OH scavenging by Se-CDs with two different paths; (d) proposed route for the ˙OH scavenging by Se-CDs on the active site of Se doped sp^2-C.
Reproduced with permission from ref. [123].

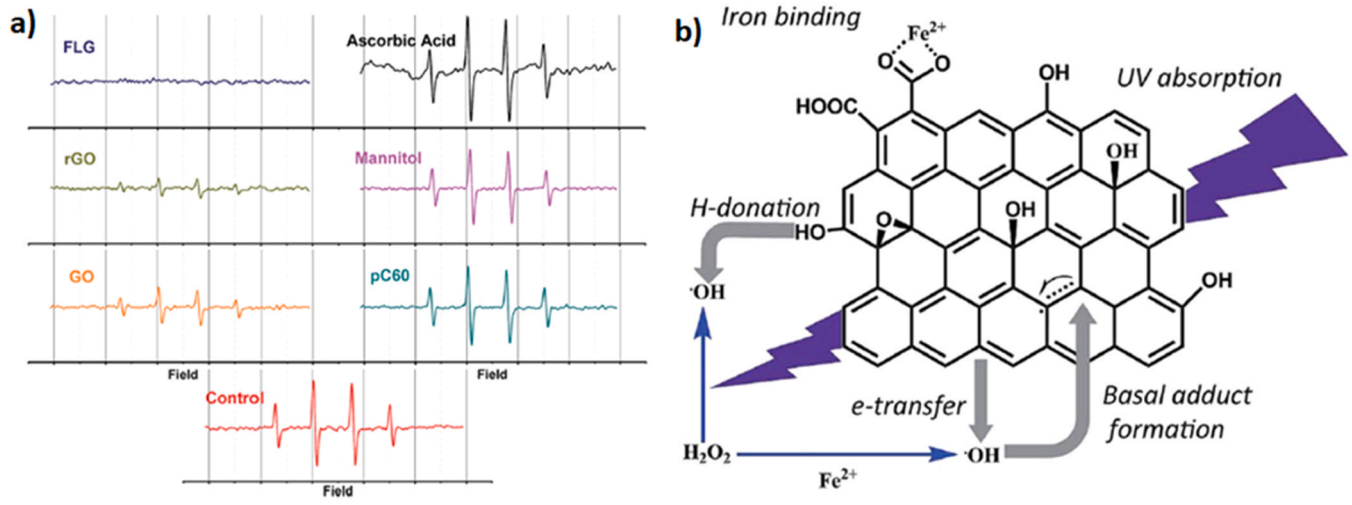

Fig. 20. a) EPR spectra of DMPO–OHc adduct formed through 20 min Fenton reaction – in the presence of 200 ppm graphene-based and reference materials. Radical scavenging potency follows rank order: FLG > rGO > GO > mannitol > pC_{60}. Ascorbic acid is a pro-oxidant under these conditions. b) Overview of relevant antioxidant mechanisms (UV absorption, iron binding, ·OH adduct formation on sp^2-carbon sites; electron transfer, and hydrogen donation). The primary antioxidant activity for graphene-based materials is against ·OH and is associated with pristine sp^2-carbon domains. Hydrogen donation activity is limited by the low population of phenolic OH, which are found on edge but not basal sites.
Rearranged with permission from ref. [93].

illumination with a blue lamp (390–470 nm) the dots produce ROS included $^1O_2$. On the other hand, when not directly exposed to visible light the C-dots mainly act as scavengers of singlet oxygen. GQDs produced by oxidation and cutting show a wider Ox-AntiOx activity, and are free radical scavengers of ·OH, $O_2^{\cdot-}$ and RNS. Illuminated by a Xenon lamp (450 nm) they generate ·OH, $O_2^{\cdot-}$ together with $^1O_2$. Similar oxidant activity is observed in Cl-doped GQDs prepared via an electrochemical method [75]. They are radical scavengers of ·OH and RNS and generators of $O_2^{\cdot-}$ (Xenon lamp 450 nm illumination). In this case, however, the formation of other ROS, such as ·OH, $O_2^{\cdot-}$ has not been observed.

In other cases the C-dots show scavenging or oxidant activity but upon addition in the synthesis of a second component they reverse the behaviour. Ox-AntiOx crossover has been measured in GQDs modified by urea or thiourea [112]. In the first case they are OH quenchers in the other one efficient generators of singlet oxygen.

C-dots obtained via microwave treatment of P-phenyldiamine can scavenge ·OH, $O_2^{\cdot-}$ radicals but after doping with Cupric (II) chloride ($CuCl_2$) with incorporation of Cu and Cl heteroatoms in the C-dots structure they reverse the antioxidant properties of pristine dots oxidants, which generate ·OH, $O_2^{\cdot-}$ and $^1O_2$ ROS under light exposure [129].

The examples reported so far are too few and the materials not enough characterized to establish a general rule for the crossover Ox-AntiOx properties of C-dots. Much more systematic work is necessary to investigate and describe the crossover capability of C-dots as a function of their structure and composition.

Conclusions and future outlooks

The comparative analysis of the data published so far shows that C-dots can be designed as both reactive oxygen species generators and radical scavengers. However, the efficiency of C-dots, either as radical scavengers or ROS generators, cannot be generalized and depends strongly on the specific type of ROS or radical. This is because the mechanisms of action differ and, therefore, the material response can be efficient only when they are specifically designed for a particular function. Proton or electron donor capability are important properties, as such as the relative content of sp^2/sp^3 sites in the C-dots. Proton donor capability is connected with the presence of different types of surface groups, such as -OH, -COOH, and -NH_2. This is not the only condition to scavenge the reactive nitrogen species because also the extent of sp^2 sites with their capability to stabilize the electronic charge and forming adducts is of primary importance. In the case of hydroxyl species the electron donor capability becomes fundamental as the presence of large sp^2 domains. Doping with electron donor atoms is a feasible option, but it is necessary to keep in mind that the antioxidation activity is given by a combination of effects. For these reasons making a clear distinction between GQSs, CQDs, CNDs and PCDs, is fundamental to design the proper antioxidant material.

Characterization of the C-dots is also critical, in particular the presence of crystalline structures should be carefully evaluated together with the relative amount of sp^2/sp^3 C bonds. The presence of functional groups should be also carefully assessed because they affect the scavenging activity of the dots.

The capability of generating ROS follows somehow a similar pattern. In this case a critical parameter is the wavelength and intensity of the light source necessary to activate the ROS. Another important conclusion is that using GQDs represents a competitive advantage with respect to other types of C-dots because of the better control that is possible to achieve.

To make an effective comparison between structure and properties, the material characterizations require more in-depth analysis with respect to what reported in most of the articles. In fact, the surface should be carefully characterized in terms of quantity and type of functional groups, in the same way it is necessary to know the extension and entity of the sp^2 domains of the C-dots as well as the extent and nature of any organized structures. Another element that must be carefully characterized is the presence of defects. These analyses in most of the works are sacrificed for the benefit of the development of applications which, however, cannot have an effective use unless all the properties of the material have been accurately characterized and understood.

The property of C-dots being able to be oxidants or antioxidants opens up many exciting prospects for practical applications. The current literature review shows that the main area of interest is likely biotechnology. C-dots have been extensively tested as a potential material for photodynamic or sonodynamic therapy. One significant application is in antiviral and antibacterial nanomaterials. In this context, C-dots can be used to create novel wound disinfection treatments and anti-biocidal systems. Another area of interest is

nanozymes, where the antibacterial properties of C-dots can be exploited in developing new generation drugs against antibiotic-resistant bacteria. Cosmetics are also a hot topic for C-dots due to the rise of anti-aging products that work by shielding the skin from free radicals, such as anti-aging creams and devices. It is also possible to use C-dots to reduce the degradation of polymeric materials under radiation. On the other hand, must be underlined that the different applications in nanobiotechnology must be associated with systematic studies on the cytotoxicity of C-dots under various conditions, which currently need to be improved.

The dual nature of many carbon dots, which act as oxidants and antioxidants, requires careful design according to the applications. The two effects can conflict, so evaluating which use and environment the C-dots will be intended for is necessary. As we have shown, the ability of carbon dots to produce distinct types of ROS can vary depending on their structure and composition, making it unlikely that a single nanoparticle can produce all the different ROS. The Ox-AntiOx properties of C-dots represent a challenging perspective for the future development of these materials. However, it should be emphasized that much more basic research is still required to control the properties fully. For the overall future of this field of research, the use of "generic" C-dots whose structure cannot be truly described and controlled represents a critical issue.

Funding

This work has been funded by eINS-Ecosystem of Innovation for Next Generation Sardinia (cod. ECS 00000038) of the Italian Ministry for Research and Education (MUR) under the National Recovery and Resilience Plan (PNRR).

CRediT authorship contribution statement

Plinio Innocenzi: Conceptualization, Methodology, Writing – original draft. **Luigi Stagi:** Writing – review & editing.

Data Availability

No data was used for the research described in the article.

Declaration of Competing Interest

The authors declare that they have no known competing financial interests or personal relationships that could have appeared to influence the work reported in this paper.

References

[1] B. Zhao, Z. Tan, Fluorescent carbon dots: fantastic electroluminescent materials for light-emitting diodes, Adv. Sci. 8 (2021) 2001977.
[2] C. He, P. Xu, X. Zhang, W. Long, The synthetic strategies, photoluminescence mechanisms and promising applications of carbon dots: current state and future perspective, Carbon 186 (2022) 91e127.
[3] J. Ren, L. Stagi, P. Innocenzi, Fluorescent carbon dots in solid-state: from nanostructures to functional devices, Prog. Solid. State Ch. 62 (2021) 100295.
[4] A. Sciortino, A. Cannizzo, F. Messina, Carbon nanodots: a review—from the current understanding of the fundamental photophysics to the full control of the optical response, C 4 (2018) 67.
[5] T. Yuan, T. Meng, P. He, Y.X. Shi, Y. Li, Xiaohong Li, L. Fan, S. Yang, Carbon quantum dots: an emerging material for optoelectronic applications, J. Mater. Chem. C 7 (2019), pp. 6820–6835.
[6] Y. Chung, J. Kim, C. Park, Photonic carbon dots as an emerging nanoagent for biomedical and healthcare applications, ACS Nano 14 (2020) 6470–6497.
[7] P. Innocenzi, L. Stagi, Carbon-based antiviral nanomaterials, graphene, c-dots and fullerenes. A perspective, Chem. Sci. 11 (2020) 6606–6622, https://doi.org/10.1039/D0SC02658A
[8] F. Yuan, S. Li, Z. Fan, X. Meng, L. Fan, S. Yang, Shining carbon dots: synthesis and biomedical and optoelectronic applications, Nano Today 11 (2016) 565–586.
[9] Rahul Bhuyan, Bramhaiah Kommula, Lopamudra Bishwal, Srayee Mandal, Santanu Bhattacharyy, From small molecules to zero-dimensional carbon nanodots: chasing the stepwise transformations during carbonization, J. Phys. Chem. C. 126 (2022) 16377–16386.
[10] T. Swift, M. Duchi, S. Hill, D. Benito-Alifonso, R. Harniman, S. Sheikh, S. Davis, A. Seddon, H. Whitney, M. Galan, T. Oliver, Surface functionalisation significantly changes the physical and electronic properties of carbon nano-dots, Nanoscale 10 (2018) 13908–13912.
[11] X. Li, M. Rui, J. Song, Z. Shen, H. Zeng, Carbon and graphene quantum dots for optoelectronic and energy devices: a review, Adv. Funct. Mater. 25 (2015) 4929–4947.
[12] F. Liu, M. Jang, H. Ha, J. Kim, Y. Cho, T. Seo, Facile synthetic method for pristine graphene quantum dots and graphene oxide quantum dots: origin of blue and green luminescence, Adv. Mater. 25 (2013) 3657–3662.
[13] M. Langer, M. Paloncýová, M. Medved', M. Pykal, D. Nachtigallová, B. Shid, A. Aquinod, A.H. Lischkad, M. Otyepka, Progress and challenges in understanding of photoluminescence properties of carbon dots based on theoretical computations, Appl. Mater. Today 22 (2021) 100924.
[14] H. Liu, X. Wang, H. Wang, R. Nie, Synthesis and biomedical applications of graphitic carbon nitride quantum dots, J. Mater. Chem. B 7 (2019) 5432–5448.
[15] H. Kang, J. Zheng, X. Liu, Y. Yang, Phosphorescent carbon dots: microstructure design, synthesis and applications panel, N. Carbon Mater. 36 (2021) 649–664.
[16] T. Zhang, J. Zhu, Y. Zhai, H. Wang, X. Bai, B. Dong, H. Wang, H. Song, A novel mechanism for red emission carbon dots: Hydrogen bond dominated molecular states emission, Nanoscale 9 (2017) 13042–13051.
[17] M. Meloni, L. Stagi, D. Sanna, S. Garroni, L. Calvillo, A. Terracina, M. Cannas, F. Messina, C. Carbonaro, P. Innocenzi, L. Malfatti, Harnessing molecular fluorophores in the carbon dots matrix: the case of safranin O, Nanomaterials 12 (2022) 2351.
[18] A. Karagianni, N.G. Tsierkezos, M. Prato, M. Terrones, K.V. Kordatos, Application of carbon-based quantum dots in photodynamic therapy, Carbon 203 (2023) 273–310.
[19] D. He, M. Yan, P. Sun, Y. Sun, L. Qu, Z. Li, Recent progress in carbon-dots-based nanozymes for chemosensing and biomedical applications, Chin. Chem. Lett. 32 (2021) 2994–3006.
[20] Y. Lv, M. Ma, Y. Huang, Y. Xia, Carbon dots nanozymes: how to be close to natural enzymes, Chem. Eur. J. 25 (2019) 954–960.
[21] S. Podder, C.K. Ghosh, A. Das, J.G. Hardy, Light-responsive nanomaterials with pro-oxidant and anti-oxidant activity, Emergent Mater. 5 (2022) 455–475.
[22] Q. Li, X. Shen, D. Xing, Carbon quantum dots as ROS-generator and -scavenger: a comprehensive review, Dyes Pigments 208 (2022) 110784.
[23] C. Xia, S. Zhu, T. Feng, M. Yang, B. Yang, Evolution and synthesis of carbon dots: from carbon dots to carbonized polymer dots, Adv. Sci. 6 (2019) 1901316.
[24] S. Zhu, Y. Song, X. Zhao, J. Shao, J. Zhang, B. Yang, The photoluminescence mechanism in carbon dots (graphene quantum dots, carbon nanodots, and polymer dots): current state and future perspective, Nano Res. 8 (2015) 355–381.
[25] P. Tian, L. Tang, K.S. Teng, S.P. Lau, Graphene quantum dots from chemistry to applications, Mater. Today Chem. 10 (2018) 221–258.
[26] A. Ghaffarkhah, E. Hosseini, M. Kamkar, A.A. Sehat, S. Dordanihaghighi, A. Allahbakhsh, C. van der Kuur, M. Arjmand, Synthesis, applications, and prospects of graphene quantum dots: a comprehensive review, Small 18 (2022) 2102683.
[27] Y. Yan, J. Gong, J. Chen, Z. Zeng, W. Huang, K. Pu, J. Liu, P. Chen, Recent advances on graphene quantum dots: from chemistry and physics to applications, Adv. Mater. 31 (2019) 1808283.
[28] S. Li, Y. Li, J. Cao, J. Zhu, L. Fan, X. Li, Sulfur-doped graphene quantum dots as a novel fluorescent probe for highly selective and sensitive detection of Fe^{3+}, Anal. Chem. 86 (2014) 10201–10207, https://doi.org/10.1021/ac503183y
[29] S. Yang, J. Sun, P. He, X. Deng, Z. Wang, C. Hu, G. Ding, X. Xie, Selenium doped graphene quantum dots as an ultrasensitive redox fluorescent switch, 6, Chem. Mater. 27 (2015) 2004–2011, https://doi.org/10.1021/acs.chemmater.5b00112
[30] B. Liu, A.J.A. Aquino, D. Nachtigallová, H. Lischka, Doping capabilities of fluorine on the UV absorption and emission spectra of pyrene-based graphene quantum dots, J. Phys. Chem. A 124 (2020) 10954–10966.
[31] J. Zhao, L. Tang, J. Xiang, R. Ji, J. Yuan, J. Zhao, R. Yu, Y. Tai, L. Song, Chlorine doped graphene quantum dots: Preparation, properties, and photovoltaic detectors, Appl. Phys. Lett. 105 (2014) 111116, , https://doi.org/10.1063/1.4896278
[32] G. Kalaiyarasan, J. Joseph, P. Kumar, Phosphorus-doped carbon quantum dots as fluorometric probes for iron detection, ACS Omega 5 (2020) 22278–22288.
[33] S. Ge, J. He, C. Ma, J. Liu, F. Xi, X. Dong, One-step synthesis of boron-doped graphene quantum dots for fluorescent sensors and biosensor, Talanta 199 (2019) 581–589.
[34] F. Qian, X. Li, L. Tang, S.K. Lai, C. Lu, S.P. Lau, Potassium doping: tuning the optical properties of graphene quantum dots, AIP Adv. 6 (2016) 075116.
[35] B. Li, X. Xiao, M. Hu, Y. Wang, Y. Wang, X. Yan, Z. Huang, P. Servati, L. Huang, J. Tang, Mn, B, N co-doped graphene quantum dots for fluorescence sensing and biological, Arab. J. Chem. 15 (2022) 103856.
[36] P. Lazar, R. Mach, M. Otyepka, Spectroscopic fingerprints of graphitic, pyrrolic, pyridinic, and chemisorbed nitrogen in N-doped graphene, J. Phys. Chem. C. 123 (2019) 10695–10702.
[37] J. Wu, P. Wang, F. Wang, Y. Fang, Investigation of the microstructures of graphene quantum dots (GQDs) by surface-enhanced Raman spectroscopy, Nanomaterials 8 (2018) 864.
[38] D. Mombrú, M. Romero, R. Faccio, A.W. Mombrú, Curvature and vacancies in graphene quantum dots, Appl. Surf. Sci. 462 (2018) 540–548.
[39] D. Pan, J. Zhang, Z. Li, M. Wu, Hydrothermal route for cutting graphene sheets into blue-luminescent graphene quantum dots, Adv. Mater. 22 (2010) 734–738.

[40] S.Y. Lim, W. Shen, Z. Gao, Carbon quantum dots and their applications, Chem. Soc. Rev. 44 (2015) 362–381.
[41] L. Zhang, X. Yang, Z. Yin, L. Sun, Review on carbon quantum dots: synthesis, photoluminescence mechanisms and applications, Luminescence 37 (2022) 1612–1638.
[42] A. Sciortino, N. Mauro, G. Buscarino, L. Sciortino, R. Popescu, R. Schneider, G. Giammona, D. Gerthsen, M. Cannas, F. Messina, β-C_3N_4 nanocrystals: carbon dots with extraordinary morphological, structural, and optical homogeneity, Chem. Mater. 30 (2018) 1695–1700.
[43] R. Ludmerczki, L. Malfatti, S. Marras, C. Carbonaro, G. Granozzi, L. Calvillo, S. Mura, I. Mandity, S. Garroni, M. Carraro, N. Senes, P. Innocenzi, Carbon dots from citric acid and its intermediates formed by thermal decomposition, Chem. Eur. J. 25 (2019) 11963–11974.
[44] Y. Song, S. Zhu, S. Zhang, Y. Fu, L. Wang, X. Zhao, B. Yang, Investigation from chemical structure to photoluminescent mechanism: a type of carbon dots from the pyrolysis of citric acid and an amine, J. Mater. Chem. C. 3 (2015) 5976–5984.
[45] Y. Xiong, J. Schneider, E.V. Ushakova, A.L. Rogach, Influence of molecular fluorophores on the research field of chemically synthesized carbon dots, Nano Today 23 (2018) 124–139.
[46] S. Tao, T. Feng, C. Zheng, S. Zhu, B. Yang, Carbonized polymer dots: a brand new perspective to recognize luminescent carbon-based nanomaterials, J. Phys. Chem. Lett. 10 (2019) 5182–5188.
[47] S. Tao, C. Zhou, C. Kang, S. Zhu, T. Feng, S.-T. Zhang, Z. Ding, C. Zheng, C. Xia, B. Yang, Confined-domain crosslink-enhanced emission effect in carbonized polymer dots, Light Sci. Appl. 11 (2022) 56.
[48] B.C. Dickinson, C.J. Chang, Chemistry and biology of reactive oxygen species in signaling or stress responses, Nat. Chem. Biol. 7 (2011) 504–511.
[49] I. Liguori, G. Russo, F. Curcio, G. Bulli, L. Aran, D. Della-Morte, G. Gargiulo, G. Testa, F. Cacciatore, D. Bonaduce, P. Abete, Oxidative stress, aging, and diseases, clinical interventions in aging, Clin. Interv. Aging 13 (2018) 757–772.
[50] S. Podder, C. Kumar Ghosh, A. Das, J.G. Hardy, Light-responsive nanomaterials with pro-oxidant and anti-oxidant activity, Emerg, Mater 5 (2022) 455–475.
[51] C. Schweitzer, R. Schmidt, Physical mechanisms of generation and deactivation of singlet oxygen, Chem. Rev. 103 (2003) 1685–1758.
[52] K.-K. Wang, S. Song, S.-J. Jung, J.-W. Hwang, M.-G. Kim, J.-H. Kim, J. Sung, J.-K. Lee, Y.-R. Kim, Lifetime and diffusion distance of singlet oxygen in air under everyday atmospheric conditions, Phys. Chem. Chem. Phys. 22 (2020) 21664–21671.
[53] Y. Ding, Q. Jia, Y. Wen, W. Liu, J. Ge, J. Wu, H. Zhang, P. Wang, New detection method for nucleoside triphosphates based on carbon dots: the distance-dependent singlet oxygen trapping, Anal. Chim. Acta 1031 (2018) 145–151.
[54] S. Maurıcio, J. Baptista, P. Di Mascio, A.A. Ghogare, A. Greer, M.R. Hamblin, C. Lorente, S. Nunez, M. Ribeiro, A.H. Thomas, M. Vignoni, T.M. Yoshimura, Type i and type ii photosensitized oxidation reactions: guidelines and mechanistic pathways, Photochem. Photo 93 (2017) 912–919.
[55] A.S. Stasheuski, V.A. Galievsky, A.P. Stupak, B.M. Dzhagarov, M.J. Choi, B.H. Chung, J.Y. Jeong, Photophysical properties and singlet oxygen generation efficiencies of water-soluble fullerene nanoparticles, Photochem. Photobiol. 90 (2014) 997–1003.
[56] P. Mroz, G.P. Tegos, H. Gali, T. Wharton, T. Sarna, M.R. Hamblin, Photodynamic therapy with fullerenes, Photochem. Photo Sci. 6 (2007) 1139–1149.
[57] H.-S. Hsieh, R.G. Zepp, Reactivity of graphene oxide with reactive oxygen species (hydroxyl radical, singlet oxygen, and superoxide anion), Environ. Sci. Nano 6 (2019) 3734–3744.
[58] A.S. Adeleye, X. Wang, F. Wang, R. Hao, W. Song, Y. Li, Photoreactivity of graphene oxide in aqueous system: Reactive oxygen species formation and bisphenol A degradation, Chemosphere 195 (2018) 344–350.
[59] M. Tamtaji, A. Tyagi, Chae Young You, P. Ryan Galligan, H. Liu, Z. Liu, R. Karimi, Y. Cai, A.P. Roxas, H. Wong, Z. Luo, Singlet oxygen photosensitization using graphene-based structures and immobilized dyes: a review, ACS Appl. Nano Mater. 4 (2021) 7563–7586 8.
[60] Z. Zhu, Z. Tang, J.A. Phillips, R. Yang, H. Wang, W. Tan, Regulation of singlet oxygen generation using single-walled carbon nanotubes, J. Am. Chem. Soc. 130 (2008) 10856–10857.
[61] B. Uprety, H. Abrahamse, Semiconductor quantum dots for photodynamic therapy: recent advances, Front. Chem., Sec. Nanosci. 10 (2022).
[62] J. Ge, M. Lan, B. Zhou, W. Liu, L. Guo, H. Wang, Q. Jia, G. Niu, X. Huang, H. Zhou, X. Meng, P. Wang, C.-S. Lee, W. Zhang, X. Han, A graphene quantum dot photodynamic therapy agent with high singlet oxygen generation, Nat. Comm. 5 (2014) 4596.
[63] B.M. Dzhagarov, G.P. Gurinovich, V.E. Novichenkov, K.I. Salokhiddinov, A.M. Shul'ga, V.A. Ganzha, Photosensitized formation of singlet oxygen and the quantum yield of intercombinational transition in porphyrin and metalloporphyrin molecules, Sov. J. Chem. Phys. 6 (1990) 2098–2119.
[64] X. Li, E.-Y. Park, Y. Kang, N. Kwon, M. Yang, S. Lee, W.J. Kim, C. Kim, J. Yoon, Supramolecular phthalocyanine assemblies for improved photoacoustic imaging and photothermal therapy, Angew. Chem. Int. Ed. 59 (2020) 8630–8634.
[65] X. Nie, C. Jiang, S. Wu, W. Chen, P. Lv, Q. Wang, J. Liu, C. Narh, X. Cao, R.A. Ghiladi, Q. Wei, Carbon quantum dots: A bright future as photosensitizers for in vitro antibacterial photodynamic inactivation, J. Photochem. Photobiol. B, Biol. 206 (2020) 111864.
[66] Y.Q. Zhang, D.-K. Ma, Y. Zhuang, X. Zhang, W. Chen, L.-L. Hong, Q.-X. Yan, K. Yu, S.-M. Huang, One-pot synthesis of N-doped carbon dots with tunable luminescence properties, J. Mater. Chem. 22 (2012) 16714–16718.
[67] S. Sarkar, M. Sudolská, M. Dubecký, C.J. Reckmeier, A.L. Rogach, R. Zbořil, M. Otyepka, Graphitic nitrogen doping in carbon dots causes red-shifted absorption, J. Phys. Chem. C 120 (2016), pp. 1303–1308.
[68] X. Chen, Q. Jin, L. Wu, C. Tung, X. Tang, Synthesis and unique photoluminescence properties of nitrogen-rich quantum dots and their applications, Angew. Chem. Int. Ed. 53 (2014) 12542–12547.
[69] F. Arcudi, L. Đorđević, M. Prato, Synthesis, separation, and characterization of small and highly fluorescent nitrogen-doped carbon nanodots, Angew. Chem. Int. Ed. 55 (2016) 2107–2112.
[70] P. Innocenzi, L. Malfatti, D. Carboni, Energy transfer induced by carbon quantum dots in porous zinc oxide nanocomposite films, J. Phys. Chem. C. 119 (2015) 2838–2843.
[71] P. Duan, B. Zhi, L. Coburn, C.L. Haynes, K. Schmidt-Rohr, A molecular fluorophore in citric acid/ethylenediamine carbon dots identified and quantified by multinuclear solid-state nuclear magnetic resonance, Magn. Reason. Chem. 58 (2020) 1130–1138.
[72] K. Holá, M. Sudolská, S. Kalytchuk, D. Nachtigallová, A.L. Rogach, M. Otyepka, R. Zbořil, Graphitic Nitrogen Triggers Red Fluorescence in Carbon Dots, ACS Nano 11 (2017), pp. 12402–12410.
[73] S. Wu, R. Zhou, H. Chen, J. Zhang, P. Wu, Highly efficient oxygen photosensitization of carbon dots: the role of nitrogen doping, Nanoscale 12 (2020) 5543–5553.
[74] X. Nie, C. Jiang, S. Wu, W. Chen, P. Lv, Q. Wang, J. Liu, C. Narh, X. Cao, R.A. Ghiladi, Q. Wei, Carbon quantum dots: A bright future as photosensitizers for in vitro antibacterial photodynamic inactivation, J. Photochem. Photobiol. B, Biol. 206 (2020) 111864.
[75] L. Wang, Y. Li, Y. Wang, W. Kong, Q. Lu, X. Liu, D. Zhang, L. Qu, Chlorine-doped graphene quantum dots with enhanced anti- and pro-oxidant properties, ACS Appl. Mater. Interfaces 11 (2019) 21822–21829.
[76] Y. Xu, Ch Wang, G. Ran, D. Chen, Q. Pang, Q. Song, Phosphate-assisted transformation of methylene blue to red-emissive carbon dots with enhanced singlet oxygen generation for photodynamic therapy, ACS Appl. Nano Mater. 4 (2021) 4820–4828.
[77] Y. Zhou, H. Sun, F. Wang, J. Ren, X. Qu, How functional groups influence the ros generation and cytotoxicity of graphene quantum dots, Chem. Comm. 53 (2017) 10588–10591.
[78] H.J. Sun, A.D. Zhao, N. Gao, K. Li, J.S. Ren, X.G. Qu, Deciphering a nanocarbon-based artificial peroxidase: chemical identification of the catalytically active and substrate-binding sites on graphene quantum dots, Angew. Chem. Int. Ed. 54 (2015) 7176.
[79] Y.-Y. Liu, Nan-Yang Yu, Wen-Di Fang, Q.-G. Tan, R. Ji, L.-Y. Yang, S. Wei, X.-W. Zhang, A.-J. Miao, Photodegradation of carbon dots cause cytotoxicity, Nat. Comm. 12 (2021) 1–12.
[80] Y. Zhou, H. Sun, F. Wang, J. Ren, X. Qu, How functional groups to influence ROS generation and cytotoxicity of graphene quantum dots, Chem. Comm. 53 (2017) 10588–10591.
[81] H. Wang, M.L. Zhang, Y. Ma, B. Wang, H. Huang, Y. Liu, M. Shao, Z. Kang, Carbon dots derived from citric acid and glutathione as a highly efficient intracellular reactive oxygen species scavenger for alleviating the lipopolysaccharide-induced inflammation in macrophages, ACS Appl. Mater. Interfaces 12 (2020) 41088–41095.
[82] J. Zhang, X. Lu, D. Tang, S. Wu, X. Hou, J. Liu, P. Wu, Phosphorescent carbon dots for highly efficient oxygen photosensitization and as photo-oxidative nanozymes, ACS Appl. Mater. Interfaces 10 (2018) 40808–40814.
[83] C. Dong, Z. Ma, Y. Huang, Y. Zhang, X. Gao, Carbon dots nanozyme for anti-inflammatory therapy via scavenging intracellular reactive oxygen species, Front. Bioeng. Biotechnol. 10 (2022) 943399.
[84] B. Kong, T. Yang, F. Cheng, Y. Qian, C. Li, L. Zhan, Y. Li, H. Zou, C. Huang, Carbon dots as nanocatalytic medicine for anti-inflammation therapy, J. Colloid Interf. Sci. 611 (2022) 545–553.
[85] D. Jana, D. Wang, P. Rajendran, A. Bindra, Y. Guo, J. Liu, M. Pramanik, Y. Zhao, Hybrid carbon dot assembly as a reactive oxygen species nanogenerator for ultrasound-assisted tumor ablation, JACS Au 1 (2021) 2328–2338.
[86] Y. He, H.S. Liu, J. Yin, J. Yoon, Sonodynamic and chemodynamic therapy based on organic/organometallic sensitizers, Coord. Chem. Rev. 429 (2021) 213610.
[87] B. Geng, J. Hu, Y. Li, S. Feng, D. Pan, L. Feng, L. Shen, Near-infrared phosphorescent carbon dots for sonodynamic precision tumor therapy, Nat. Comm. 13 (2022) 5735.
[88] F. Beuerle, R. Lebovitz, A. Hirsch, Antioxidant Properties of Water-Soluble Fullerene Derivatives, in: F. Cataldo, T. Da Ros (Eds.), Medicinal Chemistry and Pharmacological Potential of Fullerenes and Carbon Nanotubes. Carbon Materials: Chemistry and Physics, vol 1, Springer, Dordrecht, 2008.
[89] K. Okuda, T. Nagano, T. Mashino, Synthesis of various water-soluble C_{60} derivatives and their superoxide-quenching activity, Fuller. Sci. Technol. 8 (2000) 127–142.
[90] I. Fenoglio, M. Tomatis, D. Lison, J. Muller, A. Fonseca, J.B. Nagy, B. Fubini, Reactivity of carbon nanotubes: free radical generation or scavenging activity? Free Radic. Biol. Med 40 (2006) 1227–1233.
[91] A. Galano, Carbon nanotubes as free-radical scavengers, J. Phys. Chem. C. 112 (2008) 8922–8927.
[92] W. Xia, H. Xue, J. Wang, T. Wang, L. Song, H. Guo, X. Fan, H. Gong, J. He, Functionlized graphene serving as free radical scavenger and corrosion protection in gamma-irradiated epoxy composites, Carbon 101 (2016) 315–323.
[93] Y. Qiu, Z. Wang, A.C. Owens, I. Kulaots, Y. Chen, A.B. Kane, R.H. Hurt, Antioxidant chemistry of graphene-based materials and its role in oxidation protection technology, Nanoscale 6 (2014) 11744–11755.

[94] J.R. Johns, J.A. Platts, Theoretical insight into the antioxidant properties of melatonin and derivatives, Org. Biomol. Chem. 12 (2014) 7820–7827.
[95] J.L. Gázquez, A. Cedillo, A. Vela, Electrodonating and electroaccepting powers, J. Phys. Chem. A 111 (2007) 1966–1970.
[96] R. Knispel, R. Koch, M. Siese, C. Zetzsch, Adduct formation of OH radicals with benzene, toluene, and phenol and consecutive reactions of the adducts with NO_x and O_2, Ber. Bunsenges. Phys. Chem. 94 (1990) 1375–1379.
[97] Z. Haida, M. Hakiman, Food A comprehensive review on the determination of enzymatic assay and nonenzymatic antioxidant activities, Sci. Nutr. 7 (2019) 1555–1563.
[98] C.A. Ferreira, D. Ni, Z.T. Rosenkrans, W. Cai, Scavenging of reactive oxygen and nitrogen species with nanomaterials, Nano Res 11 (2018) 4955–4984.
[99] J.-J. Yin, F. Lao, P.P. Fu, W.G. Wamer, Y. Zhao, P.C. Wang, Y. Qiu, B. Sun, G. Xing, J. Dong, X.-J. Liang, C. Chen, The scavenging of reactive oxygen species and the potential for cell protection by functionalized fullerene materials, Biomaterials 30 (2009) 611–621.
[100] P. Ionita, The chemistry of DPPH· free radical and congeners, Int. J. Mol. Sci. 22 (2021) 1545.
[101] W. Brand-Williams, M.E. Cuvelier, C. Berset, Use of a free radical method to evaluate antioxidant activity, LWT–Food Sci. Technol. 28 (1995) 25–30.
[102] S. Zhao, M. Lan, X. Zhu, H. Xue, T.-W. Ng, X. Meng, C.-S. Lee, P. Wang, W. Zhang, Green synthesis of bifunctional fluorescent carbon dots from garlic for cellular imaging and free radical scavenging, ACS Appl. Mater. Interf. 7 (2015) 17054–17060.
[103] B. Das, P. Dadhich, P. Pal, P.K. Srivas, K. Bankoti, S. Dhara, Carbon nanodots from date molasses: new nanolights for the in vitro scavenging of reactive oxygen species, J. Mater. Chem. B 2 (2014) 6839–6847.
[104] A. Bayat, S. Masouma, E.S. Hosseini, Natural plant precursor for the facile and eco-friendly synthesis of carbon nanodots with multifunctional aspects, J. Mol. Liq. 281 (2019) 134–140.
[105] D. Yang, L. Li, L. Cao, Z. Chang, Q. Mei, R. Yan, M. Ge, C. Jiang, W.-F. Dong, Green synthesis of lutein-based carbon dots applied for free-radical scavenging within cells, Materials 13 (2020) 4146.
[106] A. Sachdev, P. Gopinath, Green synthesis of multifunctional carbon dots from coriander leaves and their potential application as antioxidants, sensors and bioimaging agents, Analyst 140 (2015) 4260–4269.
[107] C. Murru, R. Badía-Laíño, M.E. Díaz-García, Synthesis and characterization of green carbon dots for scavenging radical oxygen species in aqueous and oil samples, Antioxidants 9 (2020) 1147, https://doi.org/10.3390/antiox911114
[108] Y. Chong, C. Ge, G. Fang, X. Tian, X. Ma, T. Wen, W.G. Wamer, C. Chen, Z. Chai, J.-J. Yin, Crossover between anti- and pro-oxidant activities of graphene quantum dots in the absence or presence of light, ACS Nano 10 (2016) 8690–8699.
[109] J.-S. Lin, Y.-W. Tsai, K. Dehvari, C.-C. Huang, J.-Y. Chang, A carbon dot based theranostic platform for dual-modal imaging and free radical scavenging, Nanoscale 11 (2019) 20917–20931.
[110] X. Wang, L. Zhao, J. Hu, H. Wei, X. Liu, E. Li, S. Yang, Rational design of novel carbon-oxygen quantum dots for ratiometrically mapping pH and reactive oxygen species scavenging, Carbon 190 (2022) 115e124.
[111] R. Su, J. Shi, Y. Pu, J.-X. Wang, D. Wang, J.-F. Chen, Synthesis of ultrasmall and monodisperse selenium-doped carbon dots from amino acids for free radical scavenging, Ind. Eng. Chem. Res. 59 (2020) 16876–16883.
[112] S.P. Jovanović, Z. Syrgiannis, M.D. Budimir, D.D. Milivojević, D.J. Jovanovic, V.B. Pavlović, J.M. Papan, M. Bartenwerfer, M.M. Mojsin, M.J. Stevanović, B.M. Todorović Marković, Graphene quantum dots as singlet oxygen producer or radical quencher - The matter of functionalization with urea/thiourea, Mater. Sci. Eng. C. 109 (2020) 110539.
[113] P. Das, S. Ganguly, S. Margel, A. Gedanken, Immobilization of heteroatom-doped carbon dots onto nonpolar plastics for antifogging, antioxidant, and food monitoring applications, Langmuir 37 (2021) 3508–3520.
[114] Y. Qiu, Z. Wang, A.C.E. Owens, I. Kulaots, Y. Chen, A.B. Kane, R.H. Hurt, Antioxidant chemistry of graphene-based materials and its role in oxidation protection technology, Nanoscale 6 (2014) 11744–11755.
[115] H. Wang, D. Yu, J. Fang, Y. Zhou, D. Li, Z. Liu, J. Ren, X. Qu, Phenol-like group functionalized graphene quantum dots structurally mimicking natural antioxidants for highly efficient acute kidney injury treatment, Chem. Sci. 11 (2020) 12721–12730.
[116] V. Ruiz, L. Yate, I. García, G. Cabanero, H.-J. Grande, Tuning the antioxidant activity of graphene quantum dots: Protective nanomaterials against dye decoloration, Carbon 116 (2017) 366e374.
[117] Y. Wang, W. Kong, L. Wang, J.Z. Zhang, Y. Li, X. Liu, Y. Li, Optimizing oxygen functional groups in graphene quantum dots for improved antioxidant mechanism, Phys. Chem. Chem. Phys. 21 (2019) 1336–1343.
[118] D. Yang, L. Li, L. Cao, Y. Zhang, M. Ge, R. Yan, W.-F. Dong, Superior reducing carbon dots from proanthocyanidin for free-radical scavenging and for cell imaging, Analyst 146 (2021) 2330–2338.
[119] S.B. Nimse, D. Pal, Free radicals, natural antioxidants, and their reaction mechanisms, RSC Adv. 5 (2015) 27986.
[120] Y. Li, S. Li, Y. Wang, J. Wang, H. Liu, X. Liu, L. Wang, X. Liu, W. Xue, N. Ma, Electrochemical synthesis of phosphorus-doped graphene quantum dots for free radical scavenging, Phys. Chem. Chem. Phys. 19 (2017) 11631.
[121] E.E. Battin, J.L. Brumaghim, Antioxidant activity of sulfur and selenium: a review of reactive oxygen species scavenging, glutathione peroxidase, and metal-binding antioxidant mechanisms, Cell Biochem. Biophys. 55 (2009) 1–23.
[122] F. Li, T. Li, C. Sun, J. Xia, Y. Jiao, H. Xu, Selenium-doped carbon quantum dots for free-radical scavenging, Angew. Chem. Int. Ed. 56 (2017) 9910–9914.
[123] R. Su, J. Shi, Y. Pu, J.-X. Wang, D. Wang, J.-F. Chen, Synthesis of ultra-small and monodisperse selenium-doped carbon dots from amino acids for free radical scavenging, Ind. Eng. Chem. Res. 59 (2020) 16876–16883.
[124] Z.T. Rosenkrans, T. Sun, D. Jiang, W. Chen, T.E. Barnhart, Z. Zhang, C.A. Ferreira, X. Wang, J.W. Engle, P. Huang, W. Cai, Selenium-doped carbon quantum dots act as broad-spectrum antioxidants for acute kidney injury management, Adv. Sci. (2020) 2000420.
[125] D. Zhou, H. Huang, J. Yu, Z. Hu, Lysosome-targetable selenium-doped carbon nanodots for in situ scavenging free radicals in living cells and mice, Mikrochim. Acta 188 (2021) 223.
[126] L. Wang, Y. Liu, Zhouping, Y. Yanying, W. Hanbing, R. Guizhou, Y. Caimei, W.C. Lu, X. Wang, A ratiometric fluorescence and colorimetric dual-mode assay for H_2O_2 and xanthine based on Fe, N co-doped carbon dots, Dyes Pigments 180 (2020) 108486.
[127] Z. Markovic, V. Trajkovic, Biomedical potential of the reactive oxygen species generation and quenching by fullerene (C_{60}), Biomaterials 29 (2008) 3561–3573.
[128] I.L. Christensen, Y.-P. Sun, P. Juzenas, Carbon dots as antioxidants and prooxidants, J. Biomed. Nanotechnol. 7 (2011) 667–676.
[129] G. Getachew, C. Korupalli, A.S. Rasal, J.-Y. Chang, ROS generation/scavenging modulation of carbon dots as phototherapeutic candidates and peroxidase mimetics to integrate with polydopamine nanoparticles/GOx towards cooperative cancer therapy, Compos. B Eng. 226 (2021) 109364.

Plinio Innocenzi is full professor of Materials Science at the University of Sassari, and Director of the Laboratory of Materials Science and Nanotechnology. He has published more than 240 scientific articles on nanosciences and sol-gel and hybrid chemistry.

Luigi Stagi is a research fellow at the University of Sassari. He was Assistant Professor (RTDA) in the Department of Chemistry, Physics, Mathematics and Natural Sciences, University of Sassari (Italy) and visiting scientist at Georg-August-Universitat Gottingen (Germany). He earned the Ph.D. in Physics at the University of Cagliari (Italy). His research is focused on the structural and optical properties of low-dimensional materials, and the results have been reported in more than 50 publications in peer-reviewed international journals.